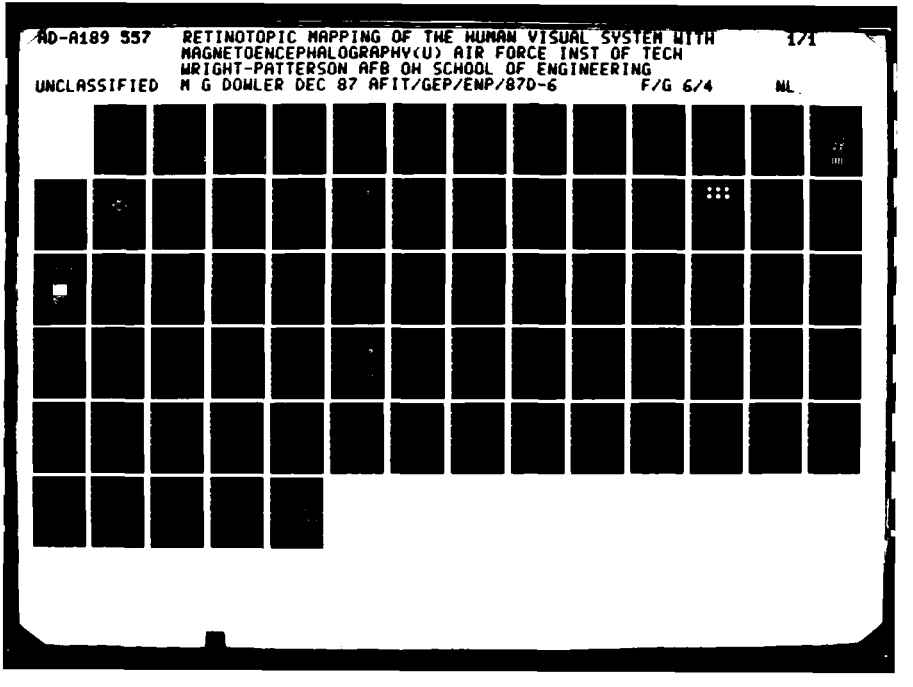
AD-A189 557 RETINOTOPIC MAPPING OF THE HUMAN VISUAL SYSTEM WITH MAGNETOENCEPHALOGRAPHY(U) AIR FORCE INST OF TECH WRIGHT-PATTERSON AFB OH SCHOOL OF ENGINEERING
1/1
UNCLASSIFIED M G DOWLER DEC 87 AFIT/GEP/ENP/87D-6 F/G 6/4 NL

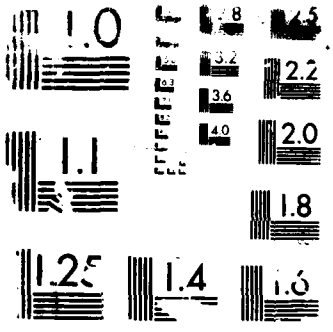
1.0
1.1
1.25
1.4
1.6
1.8
2.0
2.2

DEPARTMENT OF THE AIR FORCE

AIR UNIVERSITY

AIR FORCE INSTITUTE OF TECHNOLOGY

Wright-Patterson Air Force Base, Ohio

AFIT/GEP/ENP/87D-6

RETINOTOPIC MAPPING OF THE HUMAN VISUAL SYSTEM WITH MAGNETOENCEPHALOGRAPHY

THESIS

Michael G. Dowler
Second Lieutenant, USAF

AFIT/GEP/ENP/87D-6

Approved for public release; distribution unlimited

AFIT/GEP/ENP/87D-6

RETINOTOPIC MAPPING OF THE HUMAN VISUAL SYSTEM WITH MAGNETOENCEPHALOGRAPHY

THESIS

Presented to the Faculty of the School of Engineering

of the Air Force Institute of Technology

Air University

In Partial Fulfillment of the

Requirements for the Degree of

Master of Science in Engineering Physics

Michael G. Dowler, B.S.

Second Lieutenant, USAF

December 1987

Preface

The purpose of this study was to observe the mapping between points in the retina of the human eye to response points in the visual cortex of the brain. The technique used to observe brain activity involved measuring the magnetic field outside the head produced by electrically active areas of neurons. Since there is a point to point mapping between points in the visual field and points in the retina, a correlation was drawn between the visual field and corresponding brain area activity.

No special knowledge is necessary to understand this report. Chapter two is an in-depth look at the biological psychology of vision in order to understand some of the research that has been done in this area. The appendix is a detailed discussion of the technique of measuring the magnetic fields of the brain (magnetoencephalography) to understand brain activity. The pertinent mathematics of the technique are developed.

This study would have been insurmountable without the help of several individuals. I would like to thank my advisor, LtCol Jim Mills for thinking up the whole scheme along with the other committee members for their support, encouragement, and advice. I am especially indebted to Capt Paul DeRego for his unending interest and support throughout the entire project with all the other personnel at the magnetoencephalography and electroencephalography labs of the Aerospace Medical Research Lab. Capt Tom Dipp provided tremendous computer support and advice for which I am grateful. Lastly and mostly, I wish to thank my wife-to-be Connie Holladay for the support, advice, help, and undertanding she gave me.

"Vision is the art of seeing things invisible"--Jonathon Swift.

Michael G. Dowler

Table of Contents

List of Figures

Abstract

A retinotopic mapping was verified using magnetoencephalography as the means to observe brain activity in one human subject. The stimulus consisted of 12 sectors of a hemicircle, 6 foveal and 6 peripheral out to about 17 degrees visual field angle. The sectors flashed indiviually for 63 milliseconds with an inter-stimulus-interval between .8 and 1.8 seconds. The recording computer was syncronized to the stimulus and recorded for .5 seconds after onset of stimulus. Thirty averages were taken for each stimulus section, for each of about 45 grid points on the scalp.

The sectors were localized to distinct points in the primary visual cortex (area 17). The results did not verify the cruciform model of retinotopic mapping nor the theory that more visually eccentric stimuli produce deeper responses. The data seem to suggest a different type of mapping for foveal stimuli than peripheral, but this could also be due to the fold structure of the primary visual cortex.

RETINOTOPIC MAPPING OF THE HUMAN VISUAL SYSTEM WITH MEGNETOENCEPHALOGRAPHY

I. Introduction

This study seeks to verify a retinotopic mapping in the human visual system using magnetoencephalography (MEG) to measure specific active areas of the brain during visual stimulation. MEG consists of measuring the magnetic fields associated with neural activity in the brain, using superconducting technology to detect magnetic fields on the order of femto (10^{-15}) Tesla. The retinotopic mapping will be carried out by localizing the response of the brain to a stimulus in a small area of the visual field.

The Air Force has a great interest in advanced imaging systems. Missiles are getting "smarter" by being better able to distinguish between decoys and actual targets due primarily to advanced imaging. Robotic systems are being considered by the Air Force in hostile environments like space or chemical warfare where it is either not cost effective or too dangerous for man to do the work. These advanced robotics need advanced imaging systems in order to carry out their tasks effectively.

In order to design and build an advanced imaging system one must first understand how a successful one functions. For example, how do we perceive depth? It is of great importance for a missle or robotic system to be able to determine depth, but there are few examples of working imaging systems that can do this other than biological imaging systems.

It is largely a signal processing problem, so it is imperative to understand how the brain determines depth as well as understanding the eye's role. The hope is that by understanding how the brain processes visual information so effectively we will be better able to design efficient and effective artificial visual systems. Another area of interest is understanding how the brain perceives and recognizes patterns.

Pattern recognition is extremely useful to humans. One example is our ability to read. Could a missile be "taught" to read? In order to form an intelligent answer, we must understand a bit about pattern recognition. The first step of this is to explore what happens in our brains when we see a pattern stimulus. If we knew the exact retinotopic mapping, we could know what parts of the brain are responding to a visual stimulus of any pattern or shape. We could then look to see what happens to the image in going from the eye to the brain, or what transformations are taking place in the brain. This might give us a clue as to how the brain is able to perceive and recognize so much in an efficient manner, and a method for processing the data coming from an imaging system.

Another application of this research is that in better understanding our vision systems, we are better able to diagnose and correct problems associated with vision. If an accurate retinotopic mapping could be elucidated, biomedical scientists might be enabled to develop some sort of processing that could be done on an incoming image that would allow blind people to see.

It is clear that more research is needed in retinotopic mapping studies. The background chapter explores in greater detail research that has been done in this area.

II. Background

This chapter lays the foundation for a deeper understanding of the research problem introduced in chapter I by first delving a bit into the biological aspects of the psychology of vision and then discussing some of the previous work done in exploring this fascinating topic. The structure of the eye is first explored, followed by a discussion of the visual pathway of information. A section on human versus animal studies is next with a review of the various techniques available for studying the brain, followed by a discourse on various types of stimuli. The final section of this chapter discusses in detail pertinent studies with a bearing on the present research problem.

The Structure of the Eye

Much of the information that comes into our brains from the outside world is processed through the eyes. These vital organs have very simple optics (only one lens with an automatic aperture iris and transfer medium inside a protected ball) but very complicated muscles to move the optics and even more complicated light detectors (see figure 1). These detectors, which comprise the retina, consist of specialized cells which convert light energy into electrical activity (via a photochemical reaction) which can be processed by the brain. Only one photon is needed to convert the photopigment 11-cis-retinal into all-trans-retinal by breaking a double bond (8:129).

In the human visual system, two types of detector cells exist. Rods are sensitive to all of the visible light spectrum while three types of cones detect narrower bands of light (red, green, and blue); 120 million rods and 6 million cones make up the human retina (8:156). There is a

very dense concentration of cones in the very center of the retinal field, called the fovea, which is about 10 degrees visual field full angle (2:25).

With 126 million detectors, one would expect that the brain would be quite overwhelmed while looking at a typical full scene. This is not the case because there is a lot of pre-processing of the visual information before it even leaves the retina, as seen by the fact that the optic nerve carries fibers on the order of about .1 times the number of light detectors outside the fovea in the eye (there is a one to one mapping of detectors in the fovea to optic nerves). Retinae are actually composed of several types of nerve cells: rod and cone receptors, horizontal cells, bipolar cells, amacrine cells, and ganglion cells (see figure 2). These cells all work together to perform a process called lateral inhibition, which causes a decreased response in one receptor cell when its neighbor receptor cell has been stimulated. The effect of this pre-processing is that borders between light and dark are sharpened; for example, if within the retina a large field is evenly stimulated, then activity is greatest in the neurons connected to receptors just inside a light-dark border and smallest in those just outside the border (8:163). Likewise, every receptor cell inhibits itself, which is in part responsible for light adaptation (2:36).

The Visual Pathway

Retinotopic mapping was first verified with more simple visual systems by tracing the optic fibers from the eye to the brain. Lettvin and Maturana along with other scientists cut optic fibers from the frog brain and watched them regenerate back to their correct positions in the optic tectum of the brain (7:1709). The mammalian brain is more complex

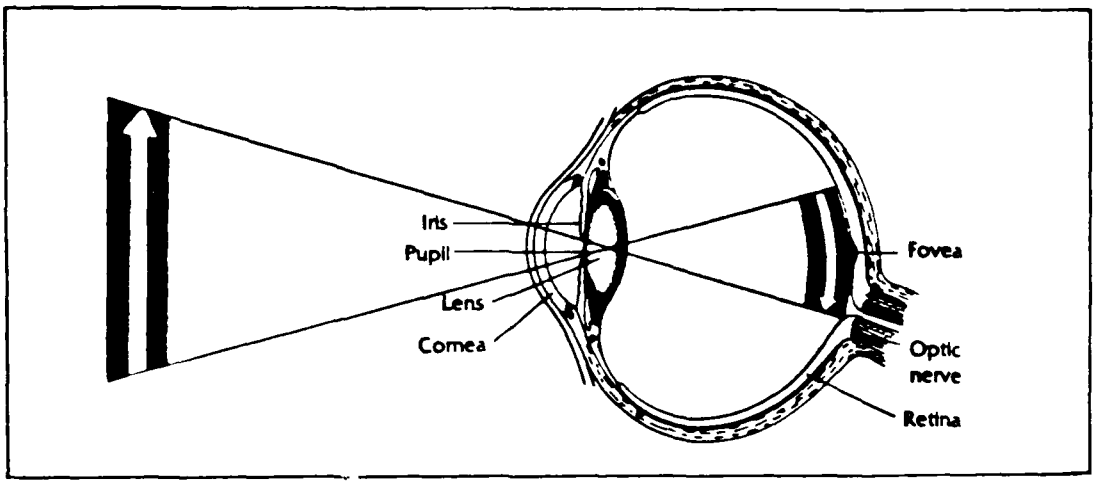

Figure 1: Structure of the Human Eye from (8:128)

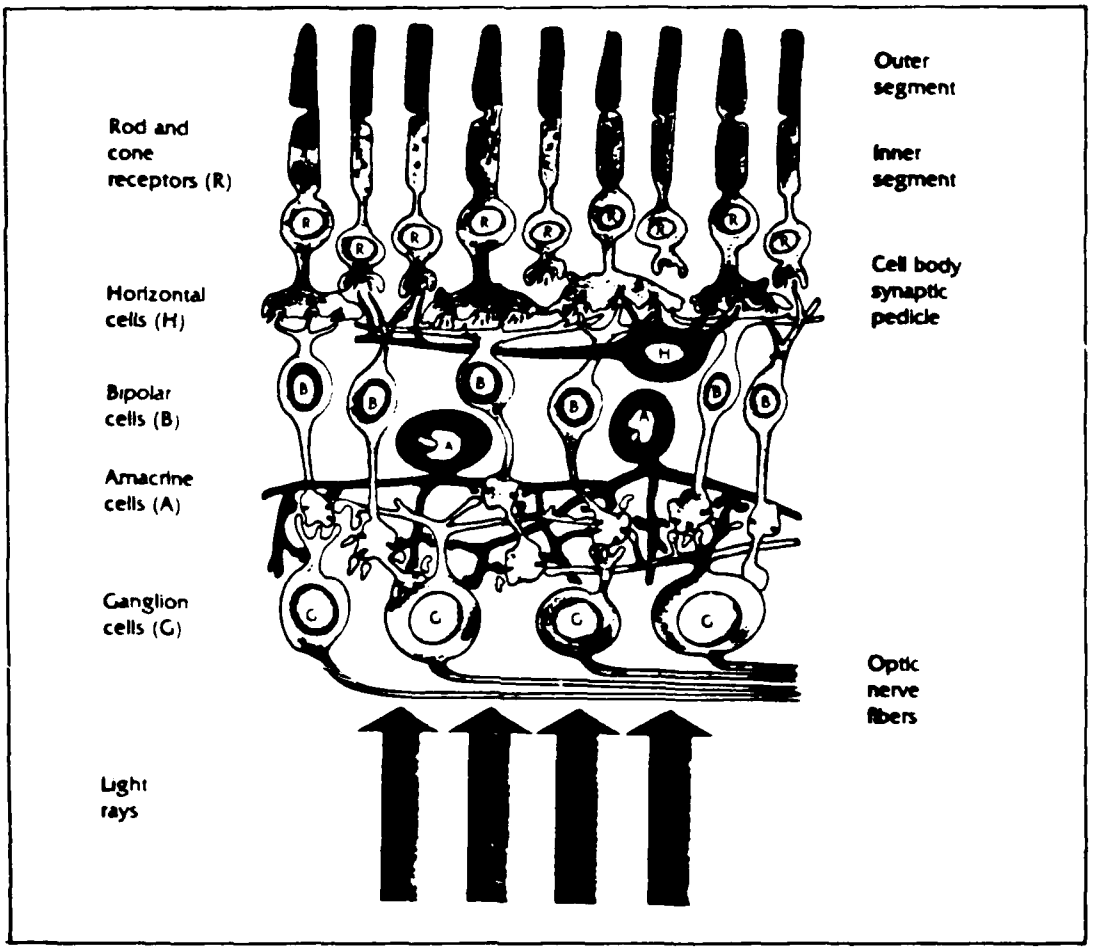

Figure 2: Nerve Cells of the Retina from (8:158)

because the signals from the eye first go through the optic chiasm where the left retinal field of the right eye crosses into the left brain and the right retinal field of the left eye crosses into the right brain. Then some of the signals go into the lateral geniculate nuclei (LGN) and on to the visual cortex in the occipital lobe, while the remaining signals go to the superior colliculi (see figure 3). This latter location is in the midbrain, an older part of the brain which roughly corresponds to the optic tectum of the frog (2:52). The role of the superior colliculus in mammalian vision is to identify where a pattern is along with basic orientation of the individual (8:174; 2:157). The LGN serve partially as switching stations and also to heighten the lateral inhibition and edge enhancement of the pre-processing in the retina, although they work on a much broader scale. The area of interest in this study is the termination of signals in the back of the brain, in the primary visual cortex. This is where more complex pattern discernment takes place as well as texture recognition (8:174).

Human Versus Animal Studies

In many of the studies mentioned in the last section of this chapter, animals were used as the subjects of investigation. Accurate localizations of cortical activity have been carried out on dogs, cats, rats, and monkeys. The choice of animal or human subjects depends on the technique involved in studying the brain and the objective of the study.

For very precise mapping studies between the retina and the visual cortex, animal studies are often preferable because one can observe the brain directly. Also, in many cases, the mapping is onto cortex tissue that may be partially hidden in folds; animal brains can be cut and

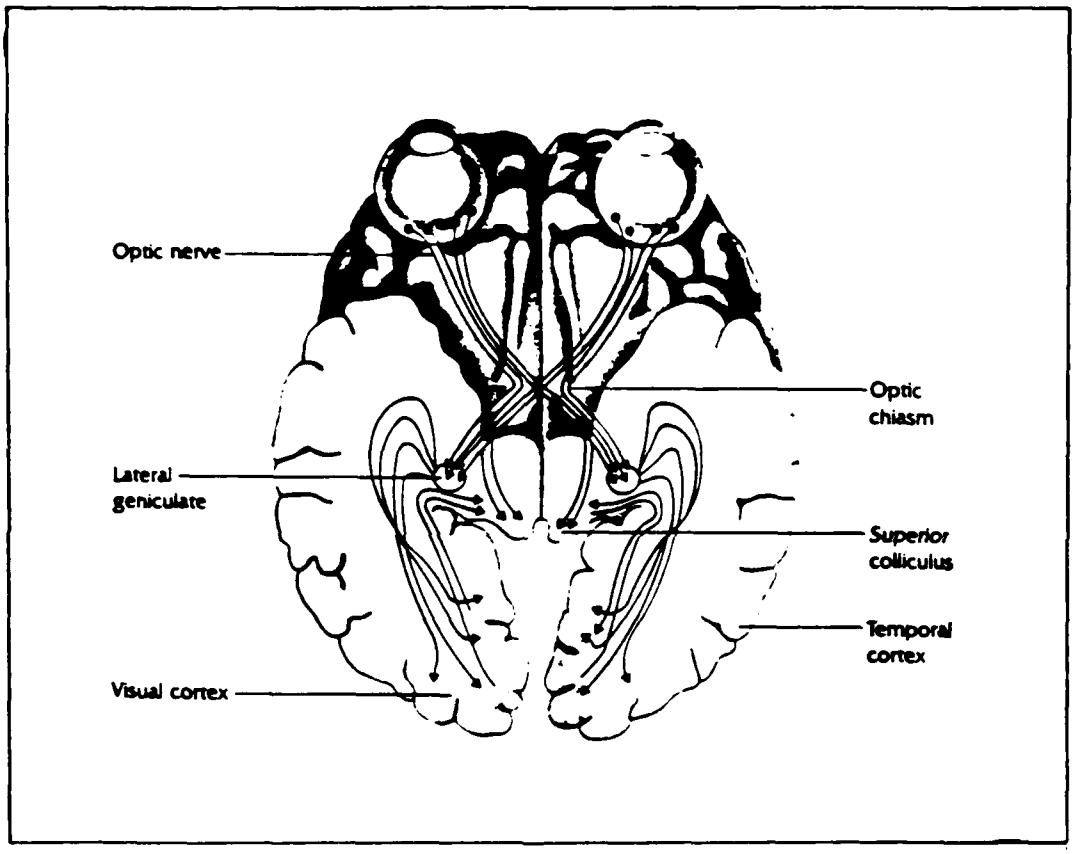

Figure 3: The Human Visual Pathway from (8:159)

smoothed out to observe the overall mapping onto the entire flat cortex. However, it is of greater interest to understand how the human brain perceives vision; although we have very similar brains to the more readily available monkeys, it is the small differences that allow us to make quantum leaps of abstraction and other higher mental abilities. So it is possible that our brains could be doing something different from the primate given the same visual stimulus. Therefore to truly understand ourselves it is desirable to study the human brain.

In the case of this study (localizing cortical activity of the primary response to a pattern stimulus) animal responses are most likely very similar to human responses because any major differences would most likely be in secondary and tertiary visual processing. Therefore it is acceptable to use some of the basic findings from some of the more pertinent animal studies to predict what the primary response of the human brain will be. Nonetheless, it is still important to observe the human brain. What is needed then, is a technique for observing brain activity non-intrusively which is still reasonably accurate for localization of cortical activity with high resolution.

Techniques

The brain has remained an enigma to man mostly because there have been few methods to actively observe living, functioning, brain tissue. Much of what we know so far has been discovered by observing brains; often the brain of a brain-damaged individual would be observed after death to correlate the area of brain damaged to the abnormality or dysfunction in behavior. With the invention of electroencephalography (EEG), milestones were made in observing living brains in a non-intrusive way. More recently, other techniques have been developed to localize

cortical activity with much higher resolution. Some of these are electrode probes, radioactive labeling, and magnetoencephalography (MEG).

Typically involving non-human subjects, the intrusive technique of inserting electrode probes into the area of interest of the brain has been used successfully to show active areas of tissue with very high resolution. These micro-electrodes are capable of measuring the current or potential of the neurons of interest directly, so the results of such a study are usually very good at indicating which areas of cortex are active.

Radioactive labeling is another intrusive technique which typically involves non-human subjects. One particular chemical used is 2-[^{14}C]deoxy-D-glucose (2DG), which is a sugar that can be taken up by active neurons in the brain. If an animal can be paralyzed or otherwise prevented from random sensory input into the brain except the input from the stimulus of interest, then the brain will absorb the radioactive chemical as the tissues absorb sugar to do work. After a time of continued stimulation, the animal can be sacrificed and the brain can be smoothed out and exposed to a photographic plate; the area of brain that was active during the stimulation will show up by darkening the plate or negative, because it is now radioactive. The reason that 2DG builds up in the neuron is because it takes much longer for the neuron to metabolize it than normal glucose. This same basic recording technique can be used on humans in positron-emission tomography (PET). Chemicals are labeled with C^{11} or F^{18} and injected into the bloodstream and eventually reach the brain. As the isotope decays, it releases gamma rays which can be detected outside the head. Imaging can be done if a large array of gamma ray detectors is used surrounding the head. One can

label glucose, oxygen, or carbon dioxide, depending on what activity is to be observed.

Electroencephalography is a non-intrusive technique for observing active areas of the brain. Used mostly on human subjects, it measures large or broad brain responses by recording gross averages of electrical potentials of the cells and fibers by means of electrodes attached to the scalp (8:214). In actuality it measures the net average of all the neurons' potentials. For example, if in one small area of brain tissue half of the neurons increase their electrical potentials while the other half decrease a comparable amount, then the net average will be zero and no change will be observed. What is of interest is the record when large numbers of cells are synchronized, as in the evoked potential method of EEG, when one uses it to measure the brain response to a sensory stimulus. The latency, or delay, between the onset of the stimulus and the response of the brain is usually constant so many responses can be averaged from many stimulus trials.

It may at this point be beneficial to explain more fully the meaning of the neuron's potential. A single neuron is composed of a cell body or soma (which includes the nucleus of the cell), the dendrites, the axon which transmits the impulse, and the terminal buttons on the end of the axon (see figure 4). The entire neuron is covered with a membrane that is selectively permeable to the passage of chemicals. This makes it possible for the neuron to have a difference in concentration of ions than with its outside world, thus being polarized; it is slightly negative with respect to outside the membrane. This initial polarization is called the resting potential and the difference between it and the outside potential is from -30 to -90 millivolts (8:37). In this resting

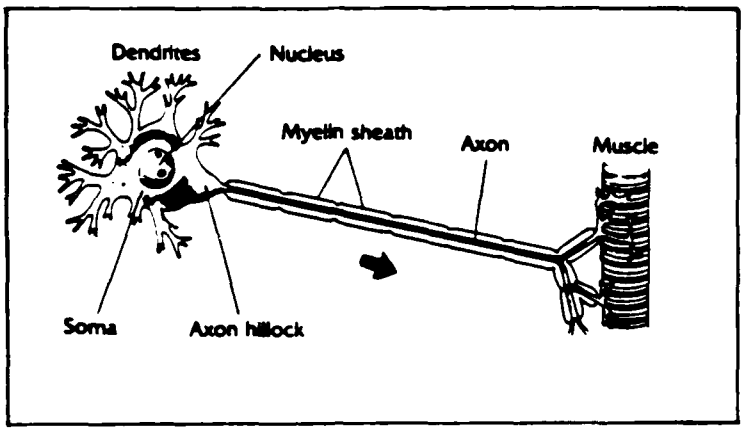

Figure 4: Major Parts of the Neuron from (8:30)

potential, the membrane of the neuron keeps potassium ions in and sodium ions out with a sodium-potassium pump which is a network of enzymes imbedded in the membrane. When the resting neuron is stimulated (usually through the dendrites on the soma) the permeability of the membrane to sodium ions changes drastically, allowing them to come into the cell. Since the sodium ions are positively charged, this negates the original negative potential inside the cell and creates a large, short lived (on the order of a few milliseconds) positive potential existing within the neuron. This potential is about 30 millivolts and travels down the axon of the neuron and conducts the nerve impulse, at a speed of about 1 meter per second in small fibers and around 60 meters per second in larger, myelinated (electrically insulated) axons (8,47). EEG detects the potential of many synchronized neurons firing. When there is a positive potential in a firing neuron and a negative potential in the rest of that neuron's axon, then an electric field exists there. This relates to the dipole theory of neuron fields. Even with this electric field, the axon is a poor conductor so that the electrical charge cannot simply conduct

down the length as in copper wire; instead, the changing permeability of the neuron membrane propagates down the length of the fiber, also propagating the action, or positive, potential.

Roth and Wikswo have calculated the magnetic field associated with the firing of a single neuron (16:93-94,107-108). This involves solving Laplace's equation for the electrical potential given the transmembrane potential, then using Ohm's law to elucidate the current density and finally Ampere's law to find the magnetic field. The magnetic field is found to be almost independent of the external conductivity of the outside medium and proportional to the internal conductivity multiplied by pi and the axon radius squared, and inversely proportional to the internal resistance on the axon per unit length (16:93).

Magnetoencephalography is the science of measuring the magnetic fields produced by the neurons of the brain in order to understand which areas are active under different conditions. It is a non-intrusive technique, typically involving human subjects. The big advantage to MEG is that it has a high degree of resolution and can give information on magnetic field sources located deep within the brain rather that just on the surface, as in EEG. The biomagnetometer itself consists of a superconducting loop in which a current is generated when magnetic flux flows through the loop, coupled to the superconducting quantum interference device (SQUID). The SQUID is composed of a superconducting loop interrupted by two Josephson junctions, and acts as a current to voltage converter with gain of about 10^7 with extremely low intrinsic noise. The entire assembly is contained in a dewar filled with liquid helium as the superconductors are made of niobium which superconducts at $9.2^{o}K$, and the dewar is suspended inside a magnetically shielded chamber which also

contains the subject. The signal is further amplified and usually constrained to a bandpass filter to eliminate the high and low frequency noise. With this type of set up, one can detect magnetic fields on the order of femto (10^{-15}) Tesla (fT); the typical visual evoked potential for a small stimulus corresponds to around 100 fT while the noise floor (on a good day) is around 20 fT. For a more complete discussion on SQUID magnetometers used in MEG see appendix A.

Stimuli

In choosing a visual stimulus for use in an MEG study, one must bear in mind the types of things that the human brain responds well to. It is more advantageous to have as many neurons firing as possible in response to a stimulus, because then one has a better chance of detecting the magnetic field over all the other brain noises. It has already been shown that the eye responds well to edges or borders of light and dark based on the neural wiring of the variety of nerve cells in the retina and also how, at the next stop on the visual pathway, the lateral geniculate nuclei further this process on a broader scale. The brain, because it has more information coming into it when the eye sees an edge, gives a larger response that is measurable with both EEG and MEG. This has been shown in various experiments using EEG; a checkerboard pattern elicited a larger response than a simply white stimulus of the same area and similar luminance. The checkerboard is also useful because one can reverse the field at a certain frequency and watch for a response of the same frequency with either EEG or MEG. By simply reversing the checkerboard pattern, the overall luminance is maintained constant, but still the eye sees a change in stimulus which is the only thing it can

respond to based on the photochemical reaction taking place during vision.

The more neurons that fire, the larger the magnetic field and the easier it is to detect the response. However, in doing a mapping of the striate cortex of the occipital lobe, one would ideally want only a point or a small cluster of neurons firing. This would enable much higher resolution, but would be impossible to detect because the magnetic field would be too so small. One then seeks a medium; a stimulus that evokes a large enough magnetic potential to detect over the other noise, but a small point so that enough points can be mapped to provide adequate resolution.

Previous Pertinent Research

By examining some of the results from earlier studies, one can gain quite a bit of insight into the problem at hand. Several excellent mapping studies have been done with monkeys, while lower resolution localizations have been performed on humans with EEG. This section is a quick review of several of these studies.

In the late 60's and early 70's, much work was done with EEG on humans using various visual stimuli. Jeffreys and Axford used an octant of a circle with a checkerboard pattern as a stimulus as well as an annular ring (6:1-21; 7:22-40). What they discovered is now known as the cruciform model (21:443). In this model, the octants of a visual field are mapped onto the cross formed by the intersection of the calcarine fissure and the longitudinal fissure (also known as the interhemispheric gap) but are transformed across the intersection (see figure 5). They also found that responses of half field stimuli were summations of two quadrant field responses or four octant field responses

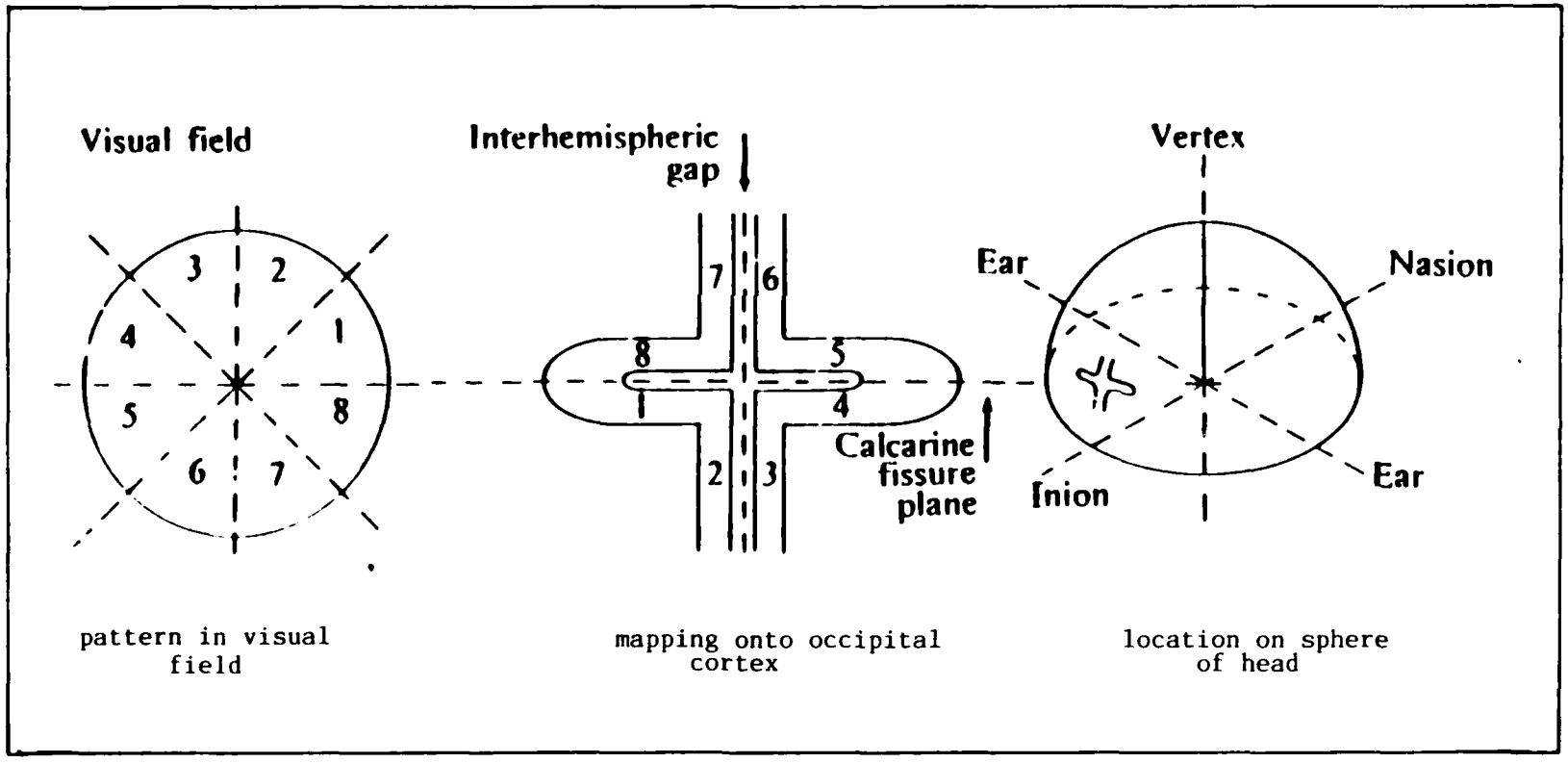

Figure 5: Cruciform Model of Retinotopic Mapping from (3:28)
originally postulated in (6:19)

(7:22) which has been verified by other researchers (3:35). Michael and Halliday did similar research on humans with EEG using a quarter-field stimulus which was either upper or lower, centered on the vertical and composed of a checkerboard pattern. They also broke this up into an inner radius and an outer radius (see figure 6). The localizations they discovered were quite broad (as is expected in EEG) and are summarized in figure 7. Both groups of researchers found that their mappings were not metrically accurate; Daniel and Whitteridge in 1961 pointed out that there was a larger cortical area devoted to the foveal as opposed to the parafoveal region, including a sort of magnification factor into their mapping of the striate cortex (3:126,127). Some other studies done with broad mappings seemed to indicate that the change in magnification factor with eccentricity was similar in all directions (3:127). Jeffreys and Axford noticed a large difference between the very inner region of the visual field and the outer portion, pointing out that "all but the very central part of the visual field is generally buried on the inner surfaces of the hemispheres...with a systematic relationship between progressively deeper cortical regions and increasingly eccentric areas of the field" (6:15). The early work done with EEG human studies showed that there was a retinotopic mapping onto the striate cortex with differences in magnification for inner versus outer areas of the visual field.

Similar work has also been done with electrode probes. Van Essen, Newsome, and Maunsell used lacquer-coated tungsten microelectrodes on macaque monkeys to observe the mapping of the visual field and found a fairly consistent retinotopic mapping along with some asymmetries, anisotropies, and considerable variation between individuals (20:429-

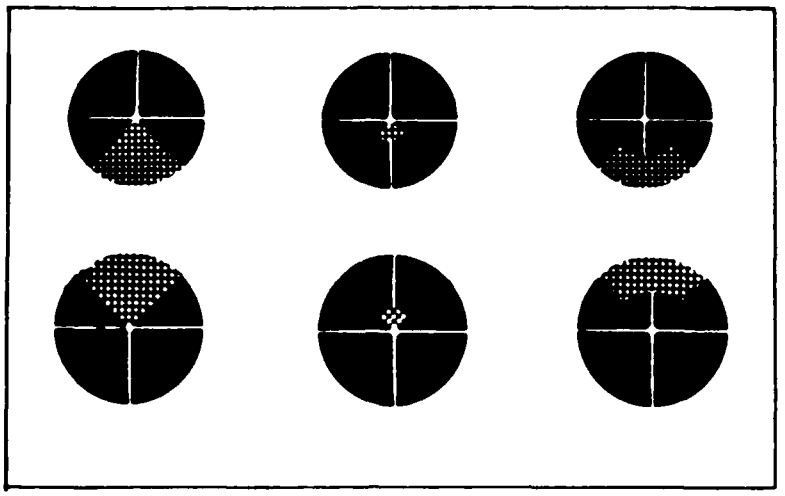

Figure 6: Stimulus from Michael and Halliday (EEG) Study from (3:122,123)

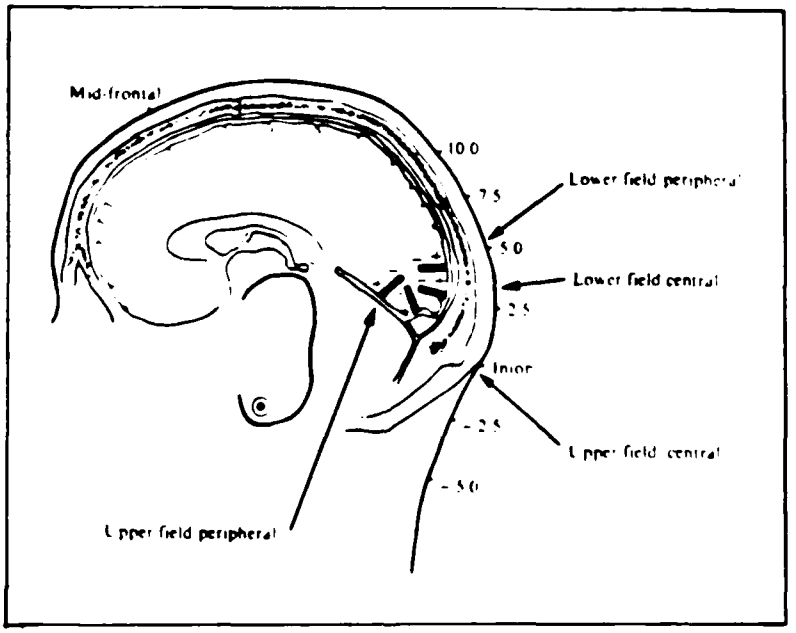

Figure 7: Localizations from Michael and Halliday (EEG) Study from (3:126)

448). They also verified an earlier theory amplified mathematically by Schwartz (17:645) who was working on the data obtained by Daniel and Whitteridge. This theory upholds a logarithmic conformal mapping as the mathematical transformation which takes place in going from the retina to the visual cortex. "In such a representation, distance in the cortex is proportional to the integral of cortical magnification" (20:437):

$$\Delta S_c \propto \int CMF$$

where ΔS_c is the distance in the cortex and the CMF is the cortical magnification factor (magnication between the retinal distance and cortical distance). Along a radius of the visual field, the magnification is inversely proportional to the distance out from the center, or eccentricity E (20:437).

$$CMF \propto 1/E$$

Then we have

$$\Delta S_c \propto \int 1/E$$

and

$$\Delta S_c \propto \ln(E)$$

where ln represents the natural logarithm. The way Van Essen, et al., assesed this transformation was to set up a stimulus as follows: a "spiderweb" of iso-eccentricity and iso-polar contour lines made up the stimulus with the animal focused on the center of the field. The contours were such that the compartments were the same shape and proportional to the square of eccentricity, or distance out from the center, in size. This distance varied as a function of the natural logarithim of the radius of the first circle. "If striate cortex

contained a true logarithmic conformal mapping, these compartments would all map onto squares of equal size in the cortex" (20:437). The stimulus and cortical mapping are shown in figure 8.

A very elegant study was done by Tootell, Silverman, Switkes and Valois which is very similar to the previously discussed study except in the technique involved. They used a 2DG radioactive chemical to trace out what parts of a monkey's brain were active after being paralyzed and shown a "wagon wheel" stimulus (19:902-904). The stimulus was set up such that there were three to five concentric rings equally spaced on a natural logarithmic scale with eight equi-angular rays. As in the Van Essen study, the idea was that if the brain did a logarithmic conformal mapping, then the areas on the mapped brain would be equal. The stimulus and results are shown in figure 9. They also found a relationship between ocular dominance and cortical magnification by noticing that the magnification factor was affected by the direction of ocular dominance strips in the striate cortex. They thus showed that the mapping was not symmetrical as had been previously observed and theorized (18:1065,1066) but rather varied with angle in the visual field.

Very little has been done with MEG and retinotopic mapping, however, Okada, et al., have investigated with MEG and visual studies. They localized a half field sinusoidal grating in the left visual field; the stimulus was reversed at a particular frequency and the SQUID magnetometer was time locked to the stimulus frequency (14:319-332; 21:443-459). Although this technique works well, it is not as good as looking for latency after the onset of stimulus (evoked potential method) because with the latter, one is looking at the entire data picture, not selective data. Their localization showed that the source was located in the right

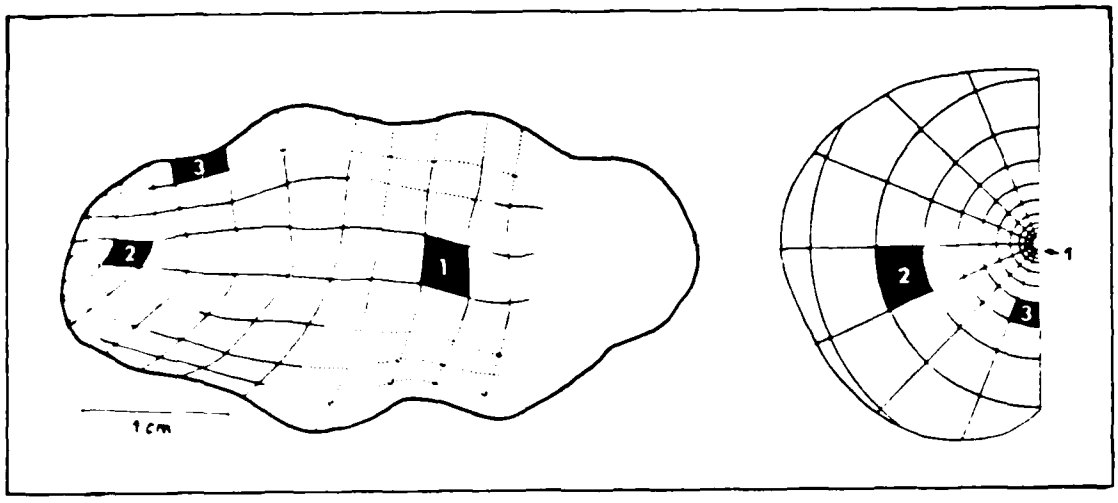

Figure 8: Van Essen (Electrode Probes) Study; Stimulus and Responses. Logarithmic Conformal Mapping in monkey, stimulus on right, mapped response on left; same area on response for log-down sized stimulus
from (20:437)

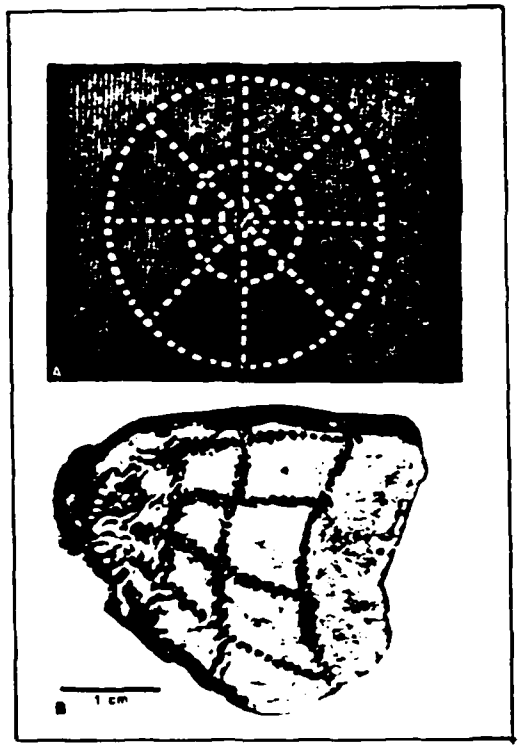

Figure 9: Tootell (2DG) Study; Stimulus and Responses.
Retinotopic mapping done with monkey using 2-deoxyglucose technique. Stimulus on top, mapped response on bottom. Equal areas in mapped diagram verify logarithmic conformal mapping, as in above figure.
from (19:902)

visual cortex. This research study was largely concerned with verifying that MEG is a valid technique for measuring brain response by comparing the MEG data with other forms of brain activity measurement, mostly EEG.

Summary

The groundwork for understanding the research problem has been laid in this chapter. First, the biological aspects of the psychology of vision were explored by discussing the structure of the eye and the visual pathway. Next, the topic of human versus non-human subjects was observed with relevancy to this experiment, followed by ideas on various types of applicable stimuli. The final section took a backward glance at some of the pertinent research done earlier, with the idea that the conclusions gained will help to design the current experimental procedures.

III. Procedures

In this chapter we come back to the problem at hand after taking a short diversion in chapter II. First, the stimulus specifications and timing are discussed. Next, a discussion of the optics used to project the stimulus into the shielded chamber and the experimental configuration of data acquisition instrumentation is presented, followed by an explanation of the recording procedures. The last 3 sections in this chapter discuss the methods of data analysis used.

Stimulus

A Commodore 64 computer running graphics enhanced COMAL generated the stimuli. Each individual stimulus consisted of a shape on a black and white cathode ray tube (CRT) monitor. The shape was either a "pie piece" or "pie piece with the front cut off" (see figure 10). With 12 shapes in all, the entire stimulus made up a hemicircle since each was 30 degrees wide and there were 6 on an inside radius (1.6 cm.) and 6 on the outer radius (8.1 cm.). A checkerboard transparency was placed over the CRT with squares of 2 mm. on a side.

The program was set up so that 6 shapes were shown in one data session, making up a quadrant of the visual field. The order of the appearance of the shapes was quasi-random, so that within a data trial a particular shape would not reappear until all the others had been shown. There was a machine language loop in the program which synchronized the COMAL program with the raster scan rate of the CRT by waiting at the proper time within the overall program until the raster was at the upper corner of the CRT before allowing the main program to flash the stimulus on. A red light-emitting-diode was taped to the front of the CRT in the

center to act as the focal point for the subject.

Each sector, as each individual pie piece stimulus will be referred to from now on, was displayed for 63 milliseconds on the screen, enough for 4 raster passes. The inter-stimulus-interval ranged from .8 to 1.8 seconds, varying because it took much longer for the graphics program to "paint" the larger sector than the smaller one. The sector was displayed only after it had been fully painted. The luminance of the smaller sector was 27.6 footlumens and the larger sector was 33.7 footlumens (297 and 362 lumens per square meter per steradian, respectively) before going through the optics.

Optics and Experimental Configuration

A CRT could not be placed inside the shielded chamber without overpowering any kind of magnetic field from the brain. The optics that were used to get the stimulus inside the shielded chamber were a simple system consisting of three convex lenses, three flat mirrors, and one orthoscopic eyepiece (see figure 11). An aperture of 3 mm diameter was inserted to improve the quality of the image, but in doing so decreased the intensity of the stimulus at the eye. The system was set up as monocular for simplicity and ease of adjustment. There is evidence from one EEG study that the binocular and monocular responses are comparable in magnitude and extremely similar in form (7:22,29-31). Also, in another study by Tootell, et al., the stimulus was only shown to one eye of the monkey in order to observe the effect of ocular dominance (19:902-904). The optical components and their mounts were made of nonferromagnetic material with each optical component being adjustable. The hemicircle outer diameter was approximately 17 degrees, and the inner diameter was all within the fovea.

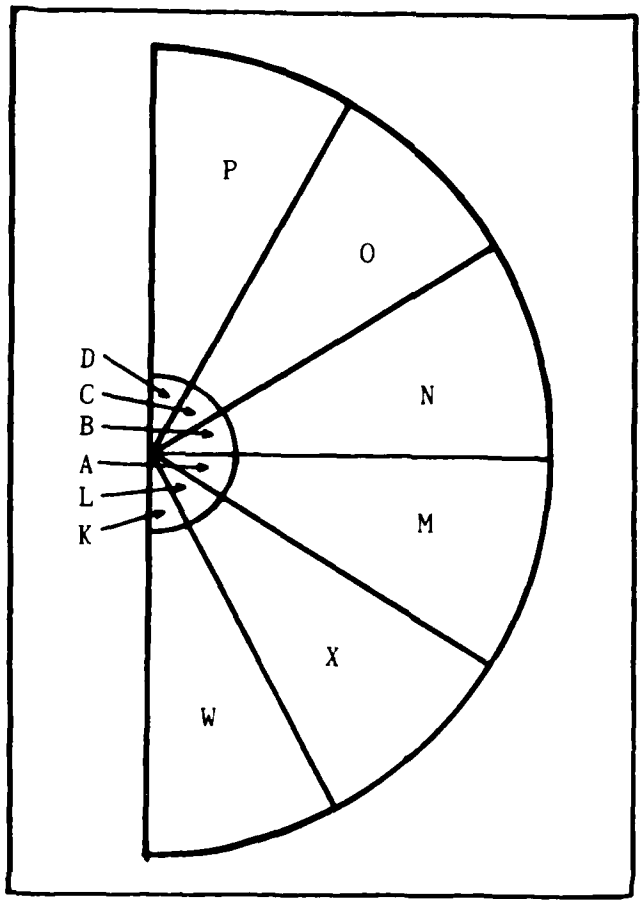

Figure 10:
The Stimulus
With Sectors
Labeled

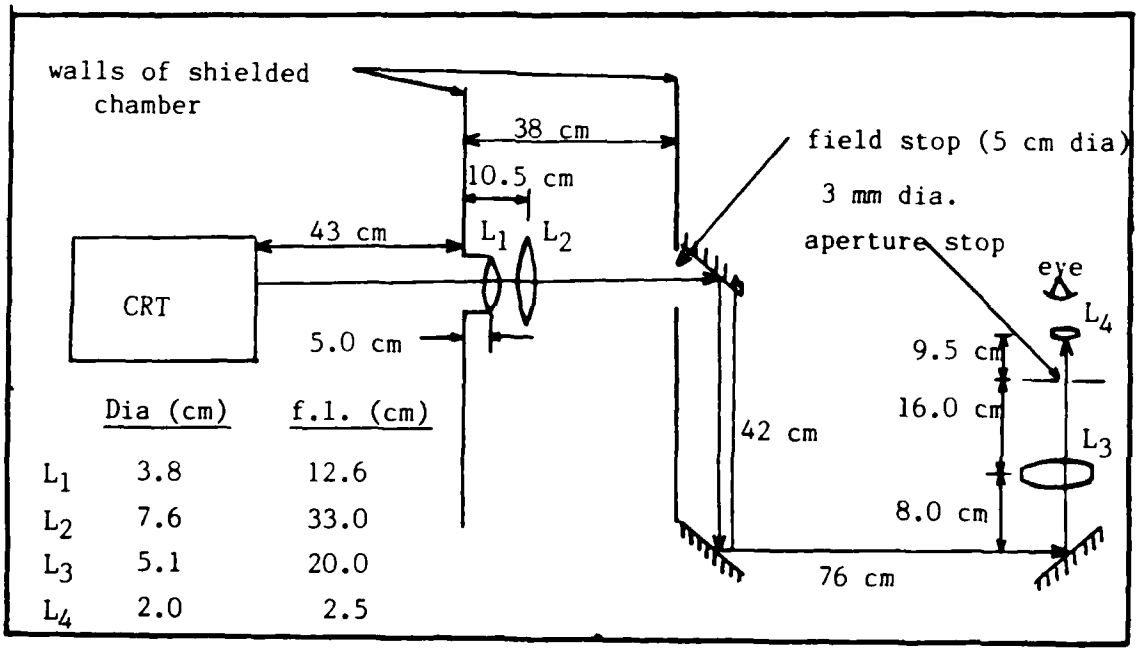

Figure 11: The Optics

The overall experimental configuration is shown in figure 12. The output from the SQUID went through a Grassamp model PF12H amplifier and bandpass filter, where it was amplified 100 times and put through a bandpass between 1 and 30 Hertz. This output was displayed on both an oscilliscope and a Nicolet signal analyzer and fast fourier transform which could monitor either the output directly on a time scale or the magnetic flux frequencies. These two devices were used to observe the SQUID output directly in real time to check for anomalies and large noise fluctuations. The output also went to the recording computer, a Masscomp 5400 which was interfaced with the Commodore in order to start recording data at the right time and store it in the appropriate Masscomp file. This was done as follows: 6 pins of the user output port on the Commodore were configured such that one pin went high (+4.5 volts) whenever the sector corresponding to that pin appeared on the screen, and this pulse was connected to the Masscomp through the analog input connectors and used as a trigger to tell the Masscomp which sector was displayed. Since each sector response was averaged over many trials, and because of the random nature of the order of appearance of the sectors, trigger integrity was very important to make sure the correct sector response was averaged with its previous responses.

Inside the shielded chamber, the subject lay on a padded bench looking down into the eyepiece with his dominant eye. Pads were used to help position the head in the most comfortable way possible and to help the subject keep his head from moving during the experiment. The bench was placed diagonally in the chamber so that the subject's head was in the center of the chamber to take full advantage of its shielding effects.

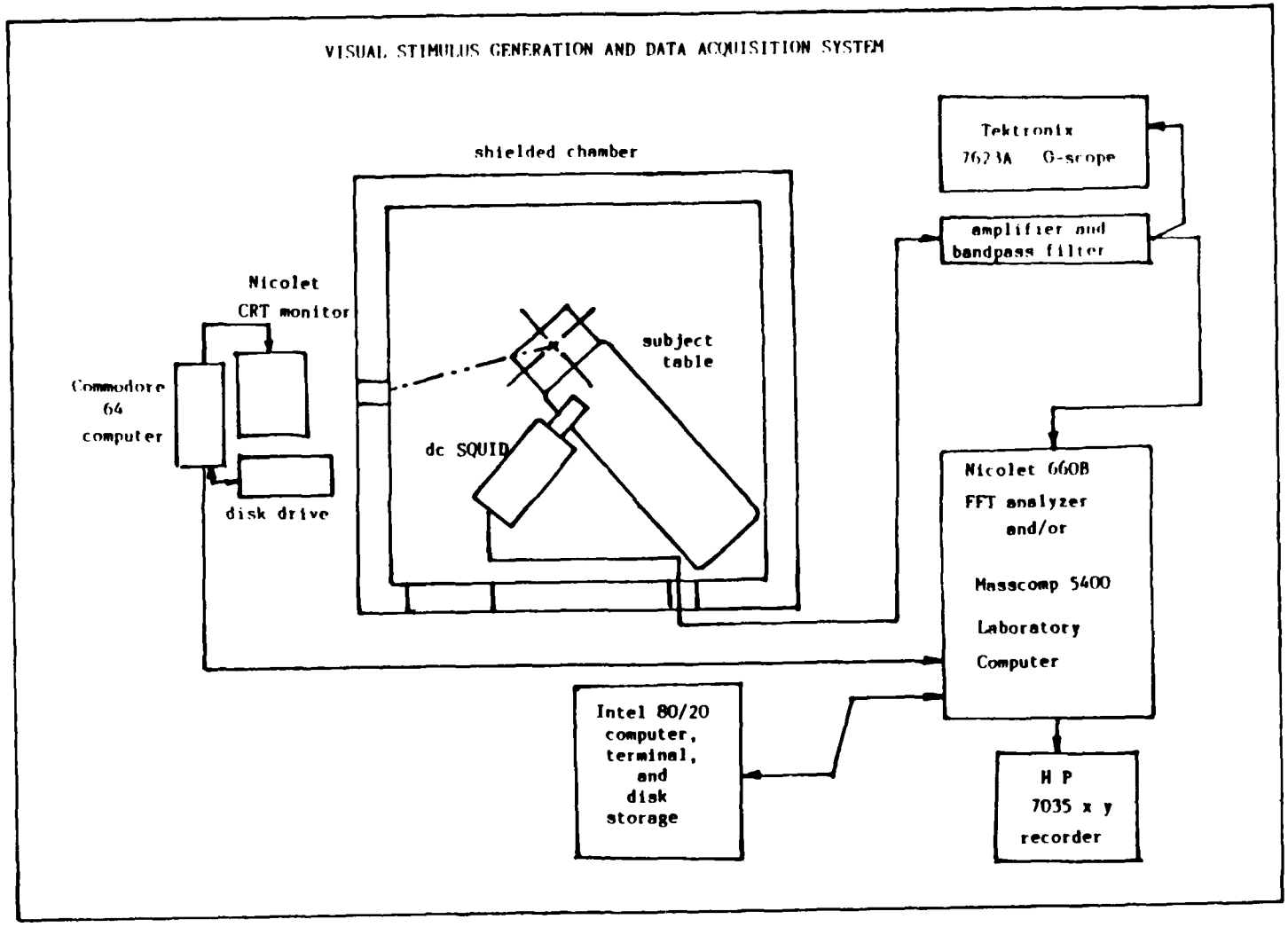

Figure 12: Experimental Configuration of MEG Lab

Recording Procedure

The subject wore a tight fitting cap which had a grid drawn on it with the inion (the small protrusion of bone on the skull just below the occipital lobe) as the zero zero (x=0, y=0) point. The grid was laid out with a centimeter as the base size, but over time this had become stretched to about 1.1 cm. The subject also wore an eyepatch over the eye not being used in the experiment so that he could keep this eye open and avoid eye strain.

The SQUID sensor was placed at a point on the grid on the subject's head tangent to the curvature of the head. A small amount of force was exerted by the sensor to push the subject into the padding to the correct postion to view the stimulus and also to keep his head from moving. During this procedure, the Commodore was running the stimulus program so that the subject could make sure his head was in the correct position to view the stimulus and also to check that it was still in focus. Then the door of the shielded room was closed and the lights turned out, and the stimulus program was stopped. Next, the Masscomp data acquistion computer was set to running and the SQUID real time output was checked, because often while moving the sensor into position the delicate electronics became disturbed from the phase locked loop required for normal operation so that the SQUID had to be reset before the recording could begin. When all was ready, the Commodore was started, causing the stimulus to start blinking while also triggering the Masscomp to take data. Thirty averages of each sector response were recorded for both quadrants for each grid point (a preliminary mapping of 40 grid points, making 80 data sessions altogether). Each data session lasted about 4 minutes and after each the subject was allowed to get up and move around.

While the Masscomp was recording the data, the averages of each sector response were displayed so that the responses could be observed. The overall recording instrument (software configuration) is shown in figure 13, and was created within the software of the data acquisition package. Input lines numbers 4 and 6 were switched to accomodate the software problem seen in the figure.

Data Analysis

Another instrument was created with the data acquisition software to play back the data (see figure 14). This included an adjustable bandpass filter, which was most often set to pass data between 2 Hertz (Hz) and 25 Hz. The data were played back one grid point and sector at a time and the latency, magnetic field strength, and sign of any peaks with a latency of 90 to 180 milliseconds that peaked above what appeared to be the noise floor were written down on a grid mapping.

The points of the grid were transformed into spherical coordinates by measuring the radius and spherical angles of each while the subject wore the cap inside a device in which a pointer could be moved to localize the grid points on the cap. As the pointer moved, one could find the angles and radius of the pointer to obtain the spherical coordinates.

Theory of a Magnetic Current Source Within A Conducting Sphere

In order to fully understand the method of calculating the depth and location of magnetic sources, one must delve a bit into the theory of a source within a conducting medium such as the brain. In 1971 Flavio Grynszpan showed in his doctoral dissertation that the magnetic field outside a conducting sphere due to a point current dipole within the

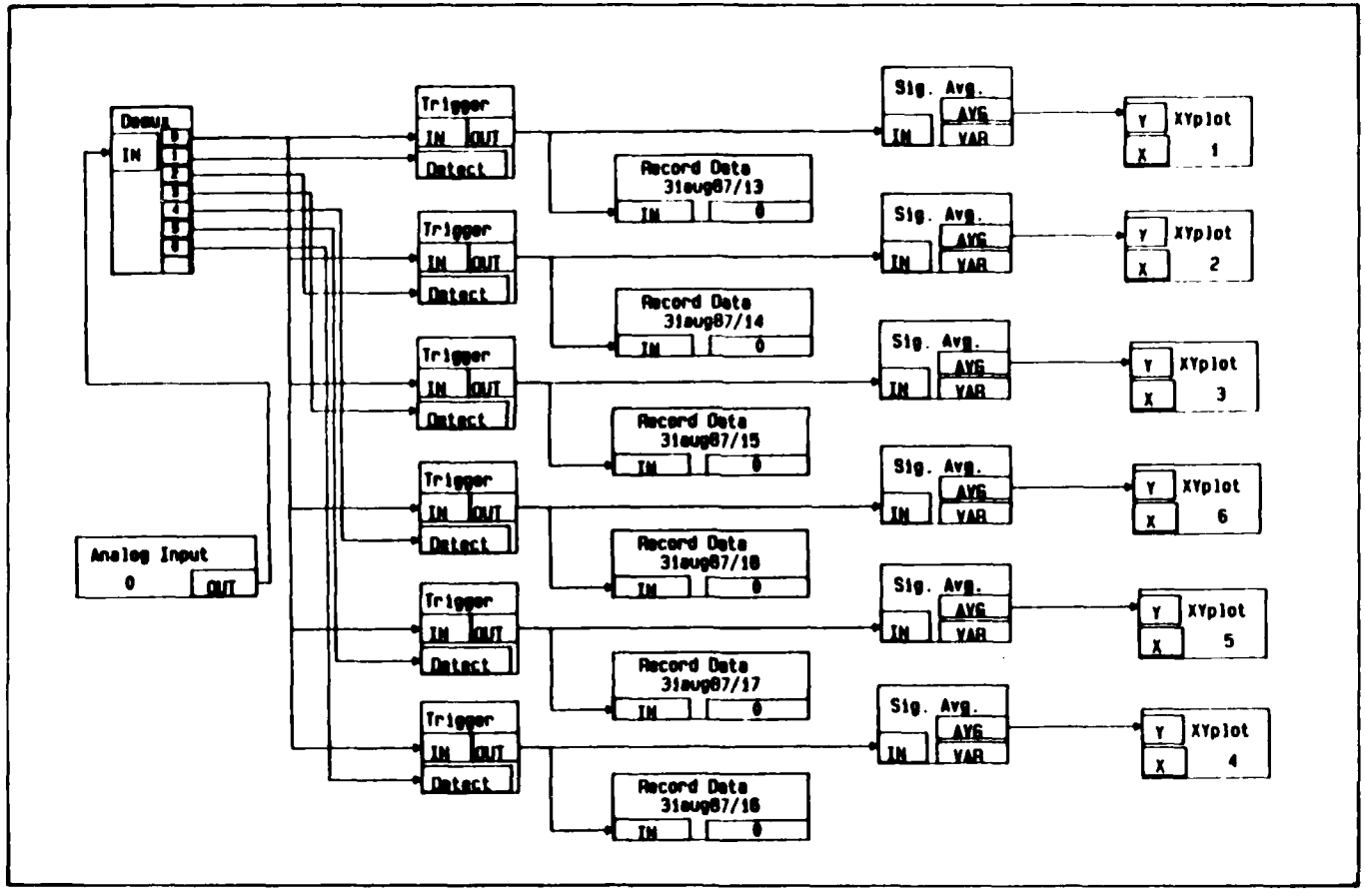

Figure 13: The Recording Instrument. Masscomp computer, Labworkbench software

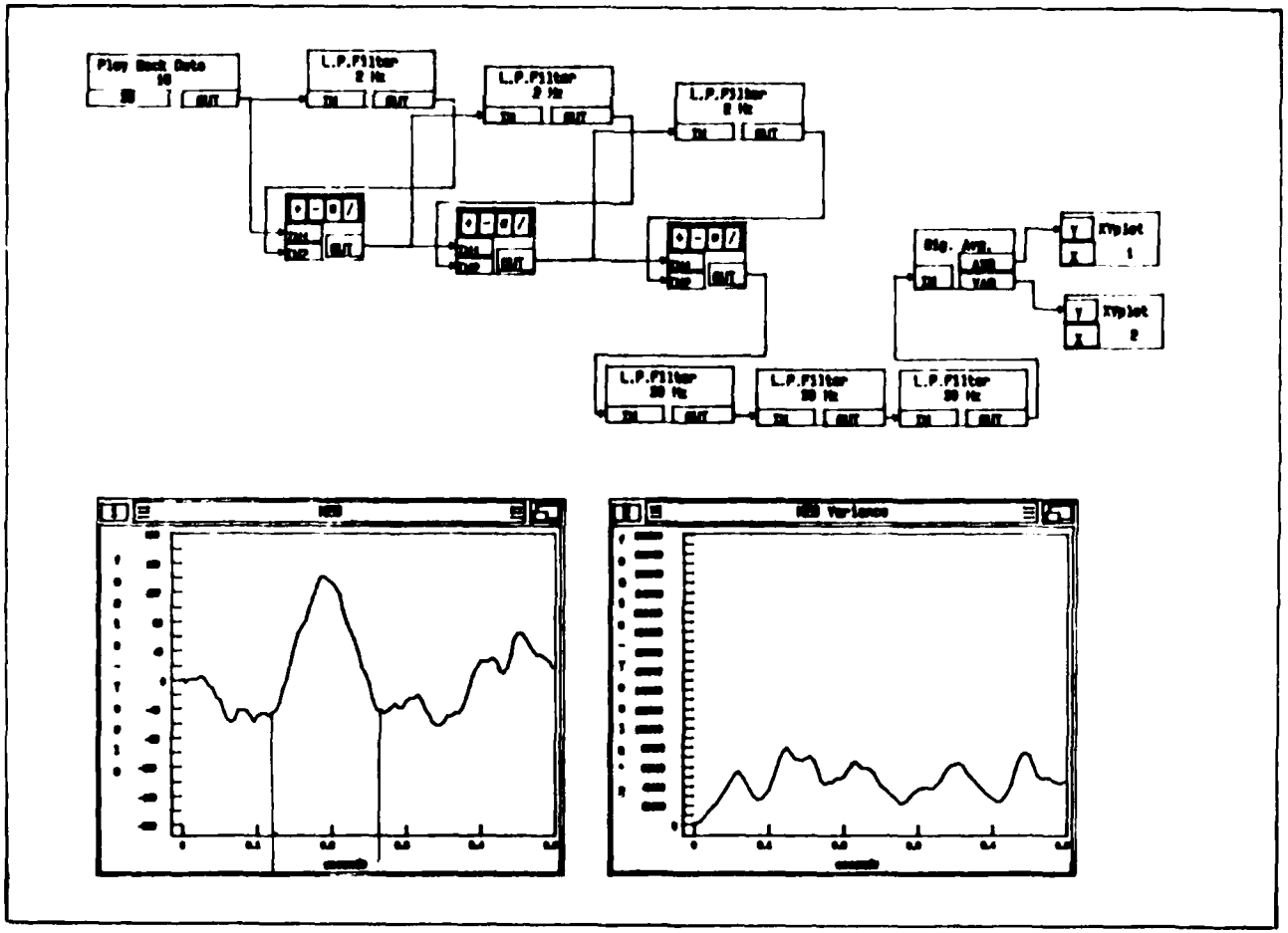

Figure 14: The Playback Instrument. Masscomp computer, Labworkbench software

sphere is independent of the radial source component (the magnetic field of the current source component oriented parallel with a radius of the sphere) (5). If then, the dipole source creating the magnetic field were completely parallel to a radius of the conducting sphere in which it existed, no magnetic field whatsoever would be detectable outside the sphere. Another result of his work was the discovery that volume currents induced within the conducting medium by the magnetic field source give no contribution to the component of the measured field normal to the surface of the conducting sphere. The practical application of this result is that if one considers the radial component of the field only, then one can completely neglect the presence of the conducting sphere.

The big advantage these results give us is that one can now consider the problem without the complexity of the conducting sphere. This allows us to fall back on simple laws of electricity and magnetism already established; if one measured the magnetic field of a point current by moving the magnetic detector around a hypothetical spherical surface, measuring only the radial component by keeping the coils of the detector tangent (flush) with the surface of the imaginary sphere, then one would expect a positive maximum and a negative maximum value of magnetic field. This is made somewhat clearer in figure 15. Since the conducting sphere makes no difference to the radial component, then these same results are expected with the source inside a conducting spherical medium.

Depth of Source

There are several different ways to determine the depth of a magnetic field source. One way is to use a computer to model the data

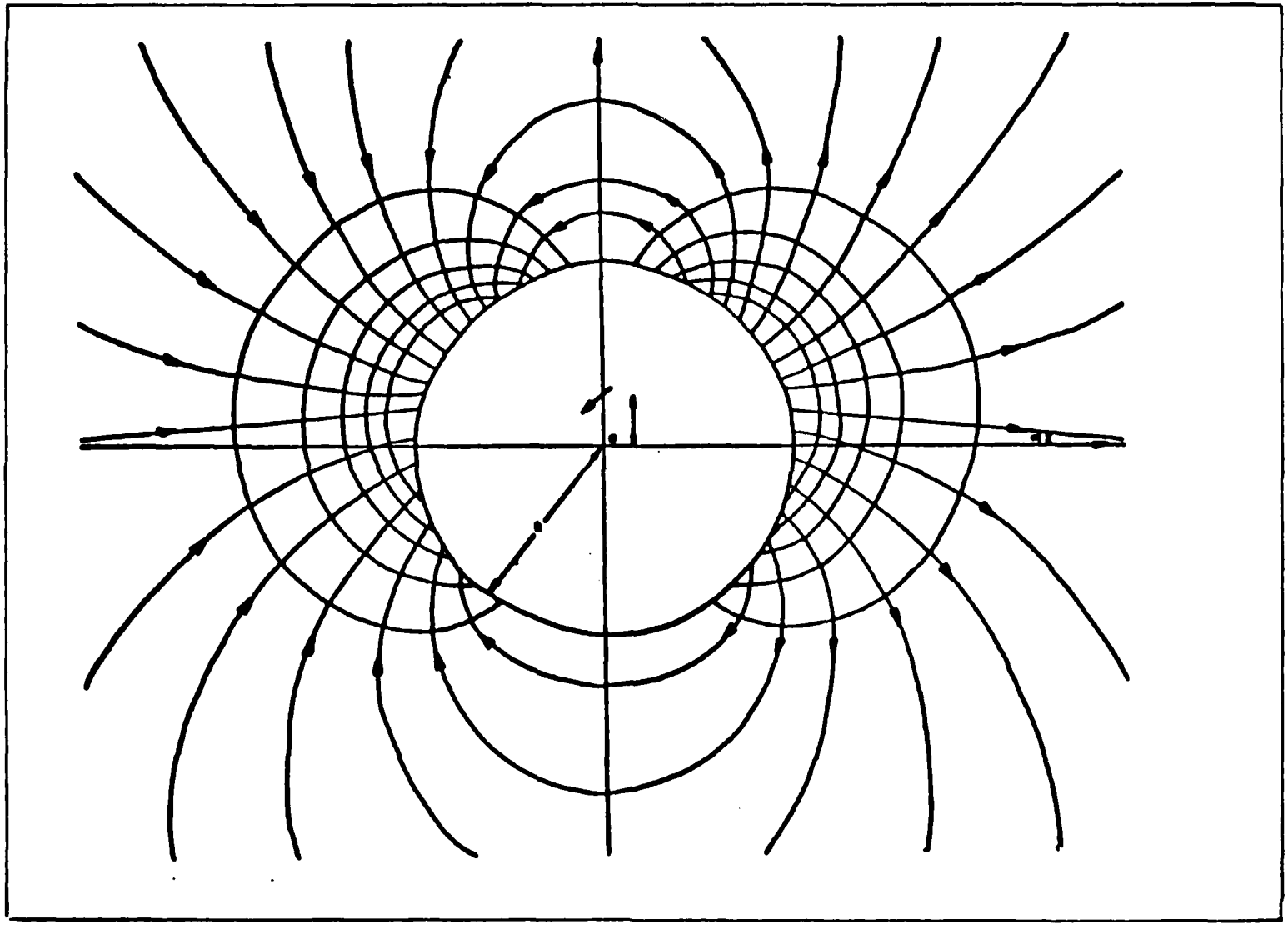

Figure 15: Magnetic Field Lines From Source in a Conducting Sphere. Notice the two points of maximum radial component magnetic field. from (5:49)

and find a best fit routine that fits the data to the model, changing the model as necessary until the data fits it within some prescribed amount.

Another method uses curves plotted for various SQUID measurement configurations. Typically, the angle separating the two maxima is plotted along the x axis in such a graph, while the ratio of the depth of the source to the radius of a best fit sphere is plotted along the y axis. The user calculates the angle of separation based on the linear distance beween the 2 points and reads off the depth. The best fit sphere is a sphere fit hypothetically into the head that gives a spherical surface over the scalp where the maxima are.

A much simpler method that can be used to determine the depth is to simply divide the linear distance separating the two points by the square root of two (9:203). This is accurate for a flat planar surface and only an estimate for a spherical surface, but is a reasonable one for the case when there is a small distance separating the two peaks. This method also assumes an infinite length gradiometer (magnetic field detection coil), that is, a single coil magnetometer as discussed in the appendix. This method very slightly underestimates the depth for a curved surface and second order gradiometer.

This chapter has investigated the procedures used in the research study in depth. The stimulus specifications were first discussed followed by the optics and experimental configuration. The recording procedures and methods of data analysis were discussed lastly, preparing for the presentation of the results in the next chapter.

IV. Results

The results of this study are best summarized by the figures and drawings of this chapter. However, some text is necessary to explain some minor results and to explain the significance and interpretation of the figures. First, the types of noise encountered in the study will be discussed followed by a description of the raw data. The first stage of data analysis, the contour plot, is discussed next with source localizations finishing up the chapter.

Noise

Many types of magnetic fluctuations which were large enough to prevent the recording of good visual evoked responses were encountered in this study. This is because the signals of interest were of small magnitude and the recording sessions were fairly long. The magnetic shielding along with the gradiometer screened out most of the external noise, but there was still a lot of biomagnetic noise. Several of these sources will be further examined, as it is imperative to reduce this noise for any further study in this area.

The first major noise source was discovered during some preliminary experiments when the subjects moved their heads slightly or tensed their neck or shoulder muscles during the recording sessions. The SQUID is extremely sensitive to movement of any kind and even the slightest movement (such as swallowing) was enough to wash out any data that might have been otherwise observed. There is a lot of magnetic activity associated with muscle contraction; when the subject tensed neck muscles, the resulting magnetic signal was quite large. This was mostly solved by placing padding that helped hold the subject's head firmly and finding a

subject that was willing to not move during the data session. Even then, the data for the lower portion of the head had more noise and uncertainty because of proximity to neck muscles.

During the preliminary experimentation, the stimulus was only one sector and larger that any later used in the study. Another source of noise was the subject's eye wandering over to where the sector was on the CRT, away from the focus point (light-emitting-diode). This was solved by introducing the random order of presentation of the different stimuli.

Rythmic responses were recorded in some subjects corresponding to brain wave activity of fairly high magnitude. Alpha wave responses were recorded in one subject of 10 - 11 Hz while in another, frequencies of 4.3 Hz were recorded, possibly corresponding to delta wave activity. Both subjects reported feeling wide awake, and further concentration on the stimulus by counting the sectors seemed to have little effect. This remains a mystery and large source of noise as nothing could be done about it without affecting the data of interest. Some of the grid points that exhibited large delta responses in the subject used in the true study were repeated with limited success.

One way to deal with noise is to set up a band pass filter that filters out high and low frequency noise. Setting the lower limit of the playback instrument on the Masscomp to 2 Hz seemed to take out a lot the noise generated by moving the SQUID by the head, while setting the upper limit to 25 Hz lessened the magnitude of the 60 Hz noise from the alternating current of the incoming power lines and also appeared to decrease the noise produced by the tensing of muscles, as this is mostly high frequency. Unfortunately, this could not be done with the rythmic brain noise as cutting this out would also have masked any viable data.

Averaging the responses would in theory remove all these noises. However, the number of averages necessary to do this would probably be greater than 50. In doing 30 averages for each sector (taking 4 minutes) the subject was hard pressed to concentrate and stay awake. Fifty averages would take around 6 minutes, which was determined to be an unacceptable length of time to minimize breathing, swallowing or blinking. Compromises were reached to decrease the noise as much as possibe. Thirty averages and a subject with minimal rythmic brain response as well as proper motivation to not move enabled conclusive data to be collected in spite of the noise.

Raw Data

An example of the raw data can be seen in figure 16. A pre-trigger of .1 second preceded the stimulus, so the latency of a response is obtained by subtracting .1 second from the value on the x axis. The average latency of the visual evoked responses for all the sectors was about 140 milliseconds (ms) with a variation of about 2 to 3 ms between different sectors.

The magnitude is read off the y axis in femto Tesla (fT). The typical response was around +/- 150 fT, often with descrepencies between positive and negative peaks, sometimes up to 100 fT.

Contour Plots

The first step in data analysis was placing the latencies and magnitudes of responses on a grid corresponding to the grid on the cap the subject wore. Twelve grids were completed, one for each sector since each sector was to be localized. If there was no response at a grid point, then null (0 magnetic field) was placed in that point; often the

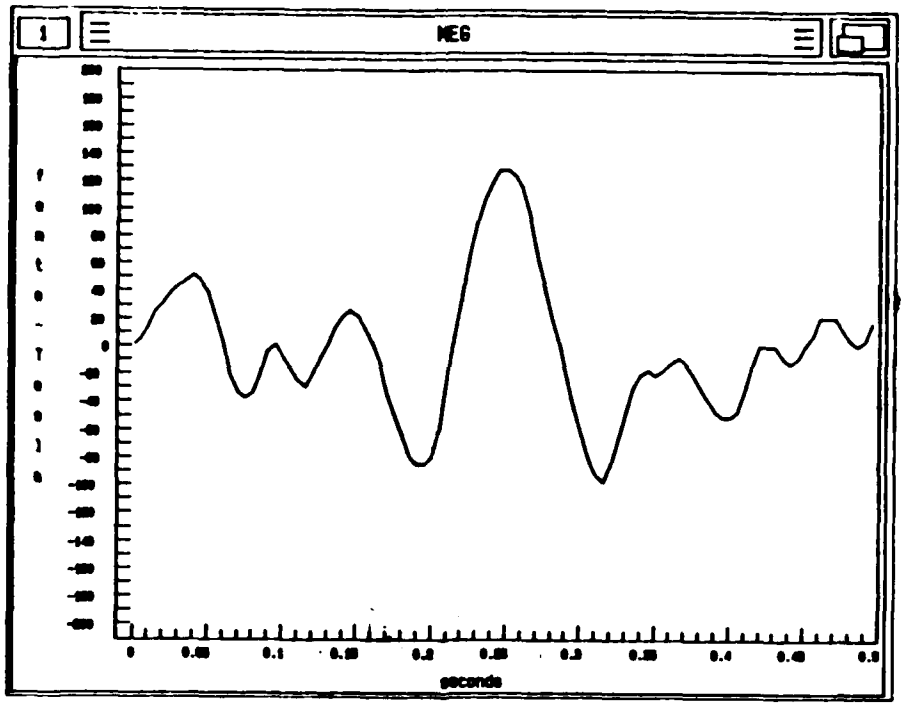

a) grid point -2,7 sector C: latency .15 sec
magnitude +130 fT

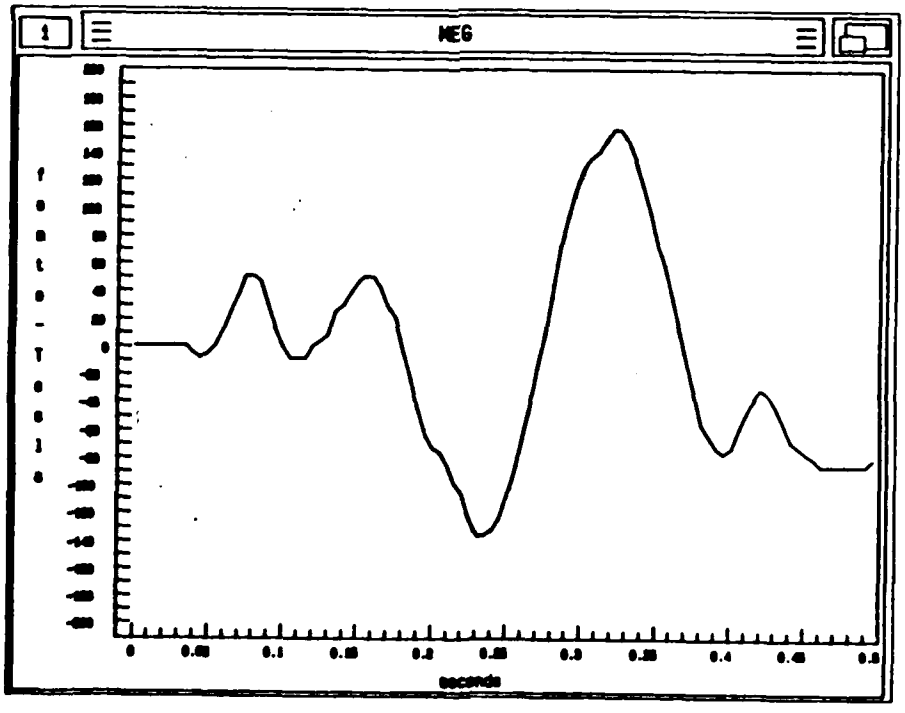

b) grid point -2,3 sector N: latency .135 sec
magnitude -135 fT

Figure 16: Example of Raw Data

value was not 0 but actually the noise floor (between about -30 and +30 fT). Other grid point values were too noisy to extract any information from. Lines were drawn by hand of constant magnetic field value (iso-field lines) resulting in a contour plot not unlike a topographic map. Several of the sector grid maps were clean enough to allow a computer to plot out the contours; these are shown in figure 17.

Localizations

As was pointed out in the last section of the previous chapter, when one measures only the radial component of the magnetic field produced by the tangential component of a dipolar source inside a sphere, one would expect to see a positive maximum and a negative maximum on the surface. All the sectors exhibited this, though some were much clearer than others. In the simplest way of localization, the source is located at the midpoint between the maxima, at a depth which is proportional to the distance that separates the peaks (1/square root of two). This method was used in this study for two reasons. At first a more accurate graph system was used as described in the procedures, but this gave source depths so shallow that they were within the skull and not brain tissue. Also, the distances separating the maxima for most of the sectors was very small, so that the surface of the head there was close to being planar. There was also so much error associated with the depth because the data on the grids was so sketchy that there would be little advantage to using an overly sophisticated approach. The depth for each sector was drawn in toward the center of the best fit sphere calculated to match the part of the head where the maxima were located. This sphere was 7 cm in radius and located 3.2 cm back from the ear canal (toward the back of the head) and 3.8 cm above it.

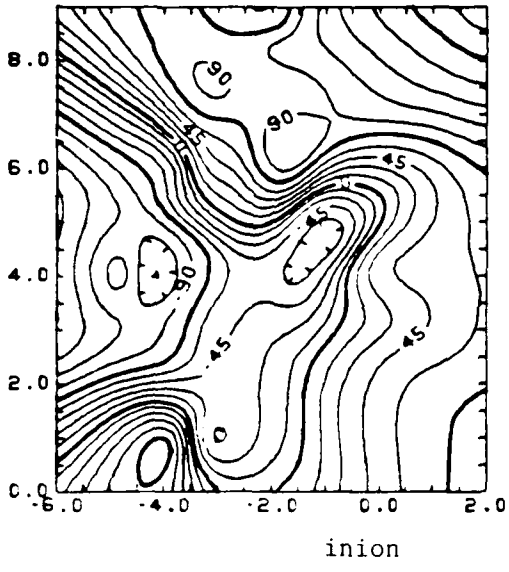

Sector D

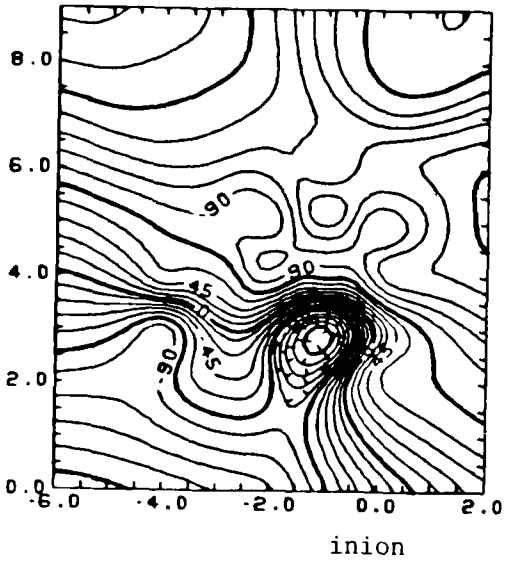

Sector L

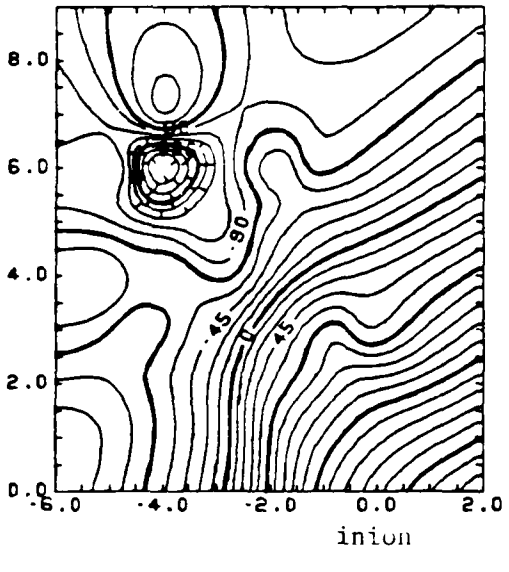

Sector W

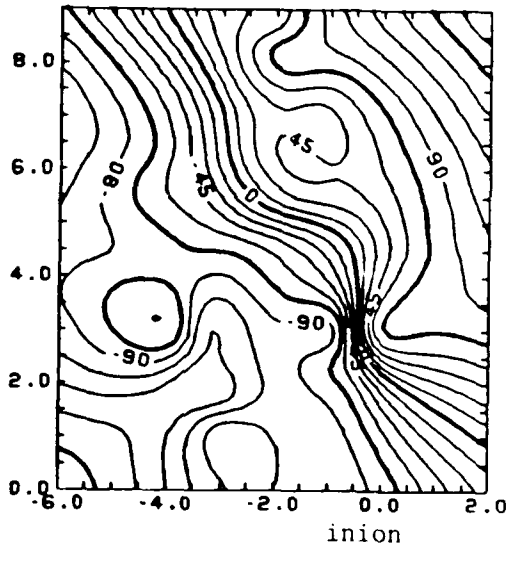

Sector X

Figure 17: Contour Plots (values in fT)

The direction of each theoretical dipole source was found by drawing a line between the two maxima and constructing a normal to this line. The source lay on the midpoint of the line connecting the maxima pointing in the direction of the normal consistent with the right hand rule. As in a current source, the thumb points in the direction of orientation while the fingers curl around the magnetic field lines. The positive maximum on the grid is where the magnetic field lines are coming out of the head while the negative maximum represents where the lines go back into the head.

Figure 18 shows the localization from two perspectives: the side view and the back view of the head. The back view perspective is slightly distorted since it is a flattening out of a curved surface. From these the 3 dimensional position of each source can be seen. The drawing is in actual size, while figures 19 and 20 have dimensions 3 times actual to show the position more closely and to give room for error curves. The error was calculated in a similar fashion to the standard deviation, because there were 2 factors which contributed to the error and compounded upon one another. The data varied a lot and quite often so that there is an uncertainty in all the localizations with more uncertainty in the sectors which had worse data (more variance, less true responses). The cap introduced another error which had to figured into the overall localization. This error was constant and was estimated by observing the variation of the grid points relative to the head each time the cap was placed on the subject. The overall error was then the square root of the sum of each individual error squared and was plotted to show the uncertainty in postion it produced.

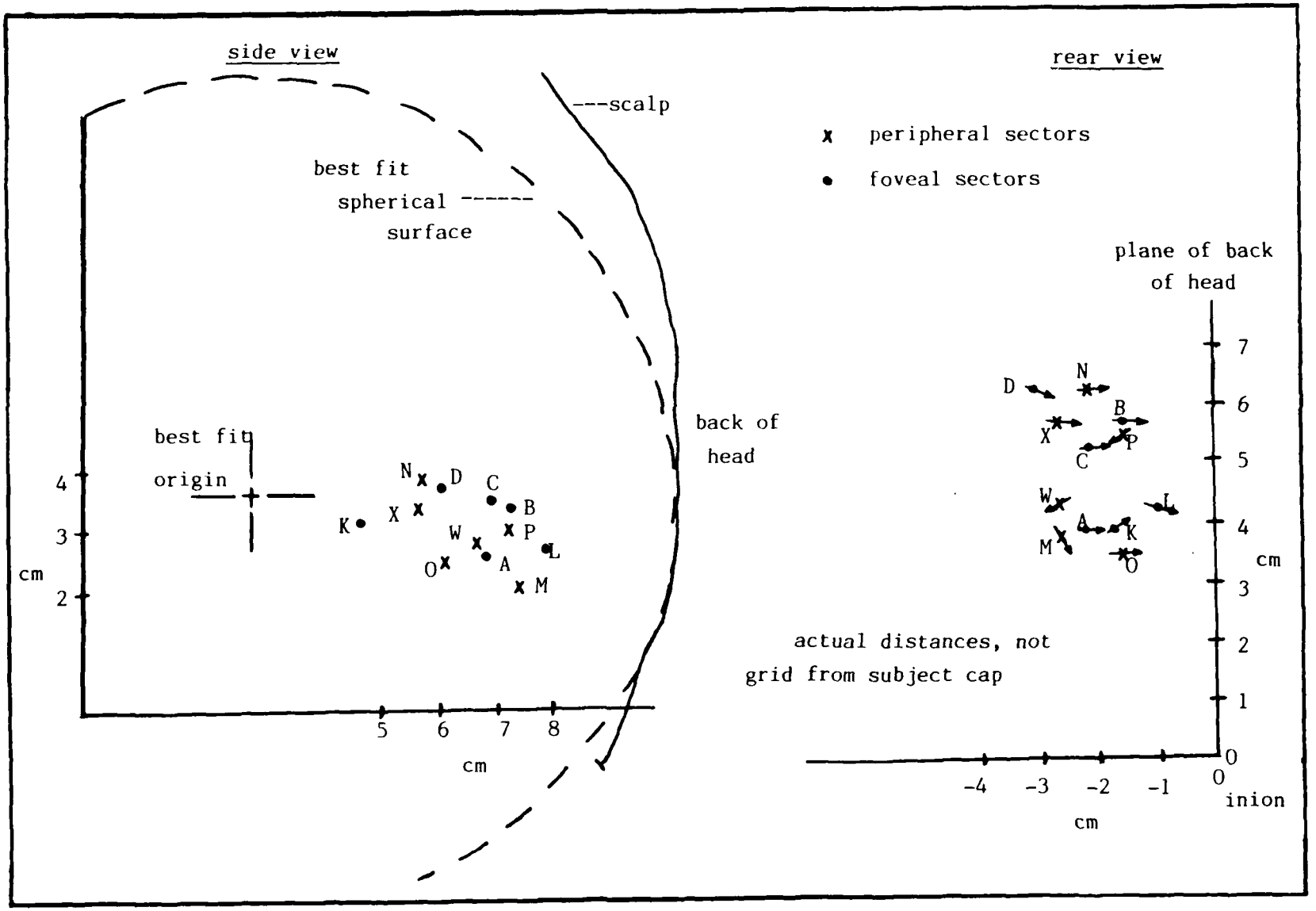

Figure 18: Source Localizations, Actual Size

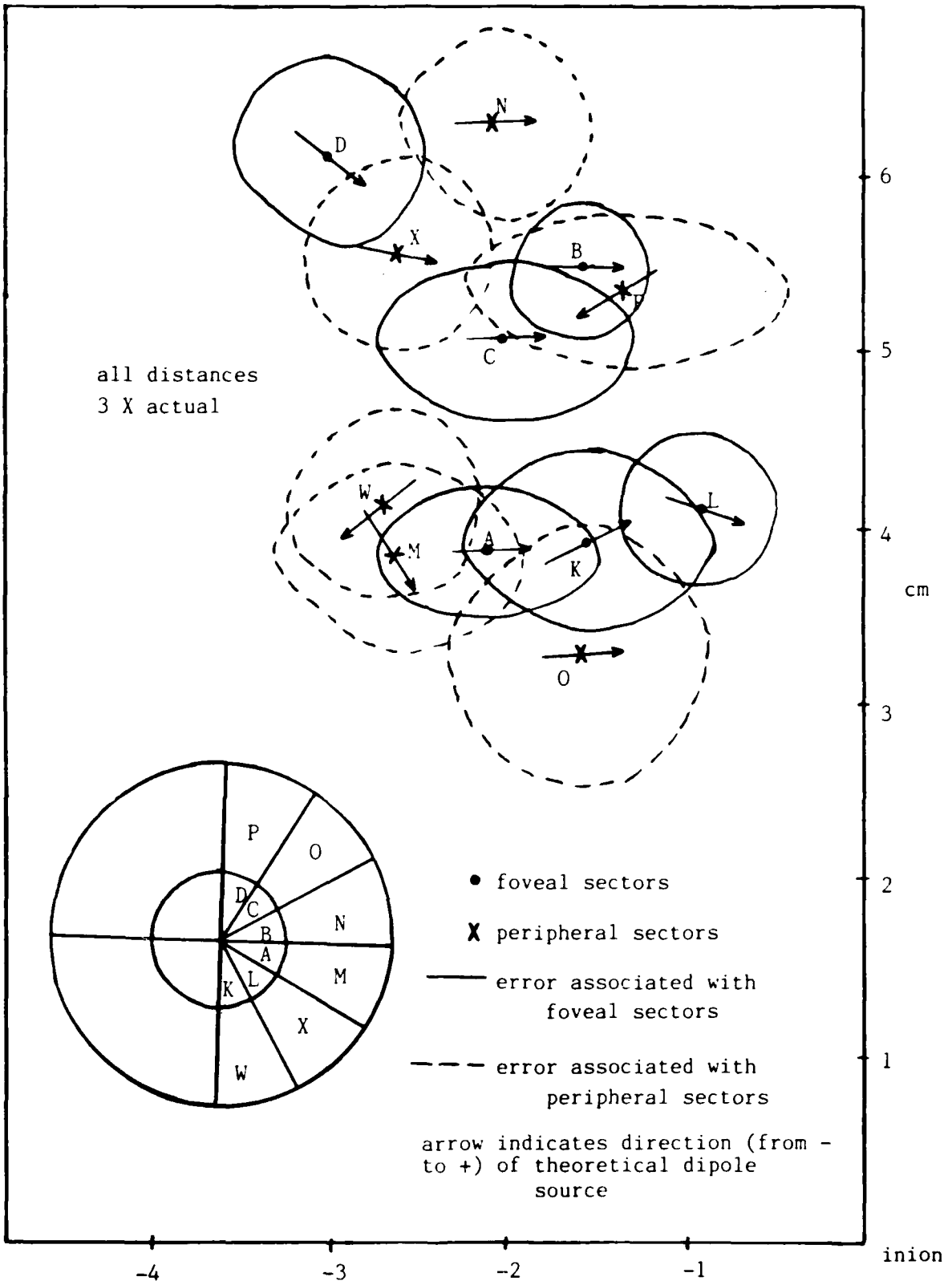

Figure 19: Source Localizations, Rear View With Error

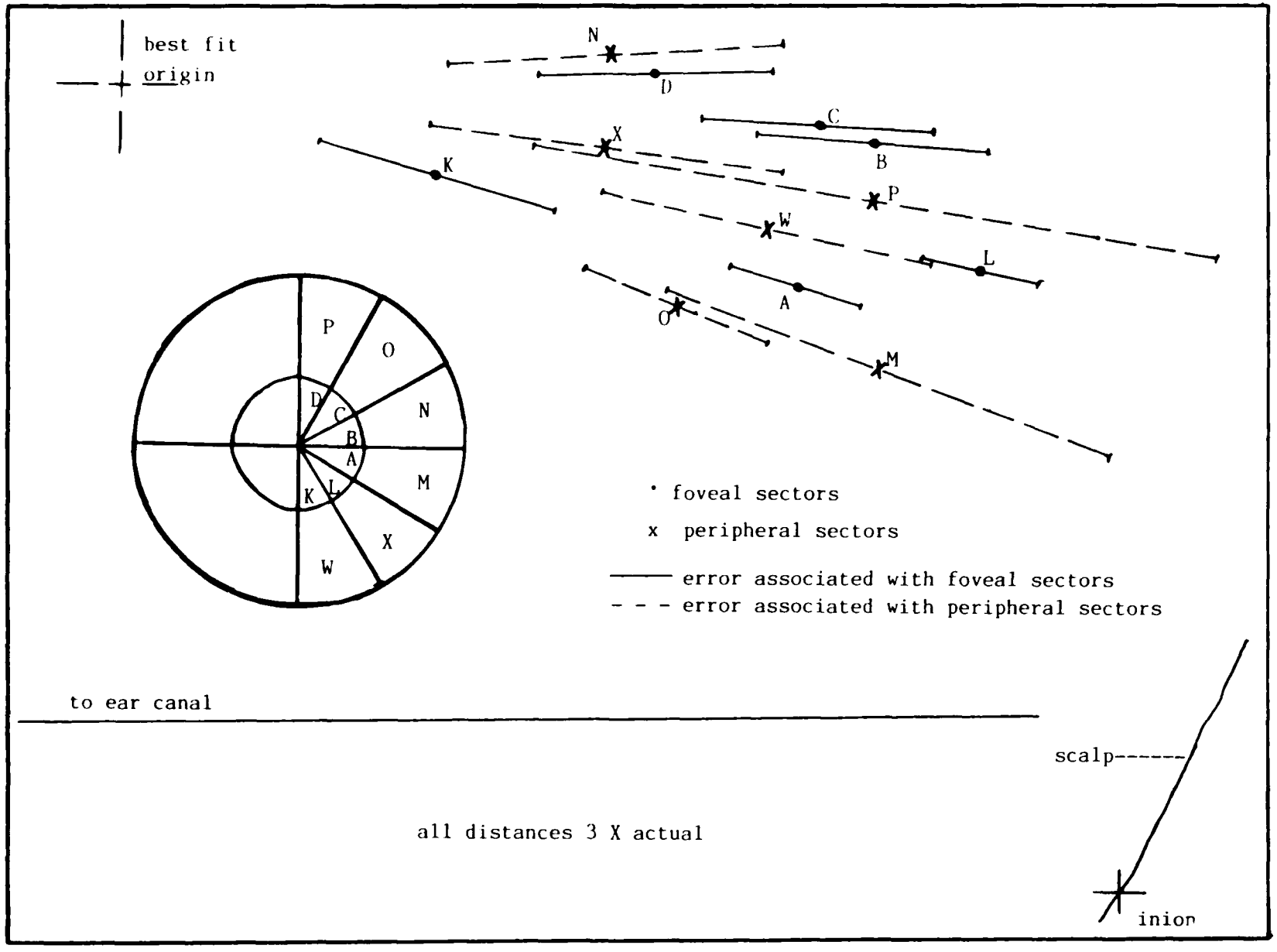

Figure 20: Source Localizations, Side View With Error (depth of localizations)

V. Discussion

In this chapter the meaning of the results and the implications relating to the human visual system will be explored. Also, validation of the results is sought by comparing these results with the products of other similar research. First, however, the noise encountered while taking data is discussed followed by an evaluation of the latencies. Next, correlation with other studies is examined with a subsequent section on unique findings, finishing off the chapter with possibilities for further study.

Noise

It was found that the subject, in trying to concentrate more on the stimulus by counting the flashes, would often become drowsy during an experimentation run. Instead of rythmic responses manifesting themselves under such circumstances as might be expected, very low noise floor levels were observed, with valid visual responses still being observed during these periods. One possibility of this is that other parts of the brain became active, away from the occipital lobe while the primary visual response was still occurring. It is possible that in trying to concentrate on the stimulus while still fully awake, the brain produces other noise in areas 18 and 19, in the secondary and tertiary visual response areas. The neck might also be tensed inadvertantly during concentration on visual stimulation, and the complete relaxation of the drowsy state reduces noise from the neck muscles as well as reduction of brain activity in adjoining areas. The occurrence of rythmic brain responses in fully alert subjects is still a mystery and will probably remain one because they vary enormously from individual to individual.

Latencies

An explanation for the diversity of latencies might involve the difference in path length from the eye to each sector localization in the visual cortex. However, a difference in .01 or .02 seconds latency would correspond to a linear difference of 30 or 60 centimeters, respectively, at a conduction speed of 30 meters per second (a rather slow approximation). This is an enormous distance in a volume as small as that which encompasses the brain, so this explanation is probably not valid. Also, the sector which had the shortest latency (M) at .12 seconds was localized the farthest away from the eye. It would seem that the sector farthest away would have the longest latency. This observation remains unexplained at present, but probably has something to do with the location of the sector in visual cortex regarding whether it is in a fold or not.

Correlation With Other Research

Previous studies have shown much about the human visual system regarding location of cortical activity as seen in chapter 2. It is of interest to compare the findings of this study to already established results to first check the validity of this research study and secondly to explore further the impact and implications of the same.

In 1982 Maclin et al. showed that the farther into the periphery the visual stimulus was, the deeper was its corresponding source location (21:446). They used MEG as the measuring technique and this result has been confirmed by other MEG researchers (9:210). The results of the present study contradict this finding; the average depth of the inner sectors was the same as the average depth of the peripheral sectors. The

studies which observed this used a different stimulus than this study, a hemi-annular stimulus placed at different angles of the visual field.

Some EEG research appears to contradict the theory that deeper sources are stimulated by more eccentric locations in the visual field. In figure 7 of the background chapter, it can be seen that the two outer stimulus localizations average to the same depth as the two inner stimulus localizations. These localizations are quite broad however, because they were elucidated with EEG. Although they agree on this point, the findings of the current MEG study appear to otherwise disagree with those of the EEG study presented in this localization diagram. For example, the lower field peripheral of this study (sector W) was localized to the middle of the response area on the visual cortex unlike at the top as in figure 7.

This study also did not confirm the cruciform model proposed by Jeffreys because in that model, the upper right visual field is mapped to the lower left of the visual cortex while the lower right is mapped to the upper left; the upper quadrant in the foveal visual field stimuli was mapped to the upper portion of cortex while the lower was mapped to the lower in the present study. The cruciform has been noted as "merely schematic" (21:443), varying significantly between individuals, so that a direct correspondence with the model is not completely expected. There is also evidence to suggest that it is possible "to resolve spatially separated sources that cannot be resolved by measuring the potentials that arise from these same sources" (9:198), pointing out that since the cruciform model was observed in EEG studies, it may be that MEG would present a slightly different mapping.

The data in the present study was inconclusive regarding the

logarithmic conformal mapping. There was not enough resolution and no information on the folds of the brain that was studied to elucidate such a mapping by the position of the mapped sectors. In theory, since the inner sectors were only .2 X the radius of the outer circle, they should have had roughly one half the area in cortex mapping and hence one half the magnitude of magnetic field strength of the outer sectors, according to a logarithmic mapping: circles with equal radii logarithmically produce equal areas in cortex. This was not observed and the information on the magnitudes is extremely varied between sectors, undoubtedly due to the fact that some were in folds and were partially masked.

A retinotopic mapping was verified because the localization of the sectors led to distinct points in the primary visual cortex. For stimuli at least the size of those used in this study, there was a one to one correspondence mapping discovered for the subject used in this study. This has extremely limited generalizations because there was not enough time to collect data that might have verified this result and only one person was used in the study.

Individual variability has been observed to be a significant factor in retinotopic mappings of primates in at least one study (20:429) and there is little reason to suspect any different with humans. We know that different people have different capabilities of perceiving 3 dimensions and that the visual cortex in infants develops differently depending on the early visual stimulation. This may partially explain why some of the previous studies are not verified by the results of this study but also limits the impact of the study to a very small margin, only one person.

Unique Findings

The single unique discovery of this study relating to retinotopic mapping is that there appears to be difference in the mapping between foveal and peripheral mappings in that the 3 upper quadrant foveal sectors were mapped fairly closely in the upper portion of the primary visual cortex and the same with the 3 in the lower quadrant, but there seems to be more randomness in the location of the peripheral sectors. Without more data on different subjects, it is impossible to tell if this is a generalizable result or merely a condition unique to the individual studied.

Possibilities for Further Study

Paramount to any additional work in this area is taking much more data with a number of different subjects. This would be most expedient with a multi-sensor SQUID; the main reason more data was not taken in the present study was because only a single-sensor SQUID was available.

A study using the same stimulus but different recording techniques would also help to prove or disprove the findings of the present study. The SQUID could be time locked to an oscillating stimulus; this would allow one to look only at the data corresponding to the stimulus. This might get rid of the rythmic noise problem because one could set the stimulus rate at a non-rythmic brain response frequency.

A major source of error which could have been avoided was in the cap used to position the SQUID. Each time the cap was put on the subject there was the possibility that the hat had stretched or that it was not in exactly the same position as before. Much more reproducible data could be taken with a SQUID sensor positioning system that would not have the variability of the cap. Perhaps a quicker solution might be a

tighter cap, such as a rubber bathing cap, or a hat made of a material that will not stretch.

A very interesting comparison would be with this data and a magnetic resonance imaging (MRI) scan of the subject to see exactly what parts of the brain relative to other brain structures are active under such stimulation. It would also be a useful check to make sure that the subject of this study had a visual cortex which matched the general population, thereby increasing the generability of this study. It may also be possible to computationally unfold the cortex with enough detailed MRI information. This might lead to a true retinotopic mapping study that is still non-invasive. One could then obtain results (at least, in theory) comparable to those obtained by Tootell and Van Essen.

One final interesting possibility might be to do a retinotopic mapping study comparing the mapping of a fighter pilot's brain to that of a concert violinist to observe the differences in visual cortex development. This might be of interest to the Air Force for determining fighter pilot standards or predicted performance under certain conditions.

VI. Conclusions

A retinotopic mapping was found using MEG as the brain activity measurement device in one human subject. The sectors were mapped onto distinct regions of primary visual cortex (area 17). There was an uncertainty in the localization of each sector which was calculated based on the estimated error from the cap and the estimated error in the data and its location on the scalp. Although this was a fairly large uncertainty in position, most of the points still corresonded to different locations in the cortex even when considering the worst case of the error.

There appeared to be differences in mapping in the foveal region compared to more peripheral areas. In the foveal area, the upper quadrant was mapped together to the upper portion of the primary visual cortex and the lower quadrant was mapped to a lower portion of cortex. The locations of the mapped sectors from the more peripheral areas of the visual field appear to be much more random in their location in visual cortex.

Appendix: Superconductive Biomagnetometers

Superconductive biomagnetometers were developed to measure the extremely small biomagnetic fields of the heart and brain, thus creating the science of magnetocardiography (MCG) and magnetoencephalography (MEG). Since this thesis studies biomagnetic fields of the brain, the measuring devices will be described from the MEG perspective. The first magnetoencephalogram was recorded in 1972 at the Massachusetts Institute of Technology to measure the magnetic field associated with the alpha wave brain pattern of a human subject. Since then, many studies have been done to further elucidate the brain's role in perception. In order to understand modern tools and techniques of MEG, two topics must first be dealt with--superconductivity and Josephson junctions, leading into the superconducting quantum interference device (SQUID), and finishing off with the overall construction of the entire biomagnetometer.

Superconductivity

Kamerlingh Onnes first discovered superconductivity in 1911, three years after first liquifying helium (15:818). He was working in Leiden with the metal mercury, when he discovered that the resistivity appeared to drop off to practically zero, or 10^{-5} ohms as he could measure it. Later, measurements were made which verified that the resistivity does indeed become zero (21:72).

The second experimental effect of interest regarding superconductors was discovered about 20 years later by Meissner and Ochsenfeld (13). They found that a magnetic field cannot exist inside a superconductor because a current is set up in a very thin surface layer such that the

outer field compensates for any inner field. This is now called the Meissner effect, and occurs regardless of whether the external magnetic field is applied above or below the critical temperature of the superconductor, that is, the temperature where the metal first starts to conduct with zero resistance.

The first satisfactory microscopic theory explaining superconductivity was published in 1957 by Bardeen, Cooper, and Shrieffer (1). Now called the BCS theory, it accounts for the interesting phenomena via a Bose-Einstein condensation. Particles which obey Bose-Einstein statistics are called bosons: they have integral spin values and do not obey any exclusion principles. Therefore, one can have as many bosons as possible in any energy state. According to the BCS theory, electrons interact with the vibrational modes (phonons) of the positive ion lattice of a superconductor resulting in a diminuation of the Coulomb repulsive force between them. When there are many such electron-phonon interactions at a very low temperature, the net observed effect is an attractive force between electrons, allowing pairs of electrons to bind with spins antialigned so that each pair (called a Cooper pair) has a net spin of zero. Because their spins are zero, they act like bosons and do not obey the Pauli exclusion principle. If one lowers the temperature on a closed set of bosons towards zero, the momenta drop to a minimal value (consistent with the uncertainty principle). The collapse of a large group of bosons to a collective ground state where they all have the same minimal ground state momenta is called a Bose-Einstein condensation. As the momentum of a particle in such a system decreases and approaches zero (hence becoming more certainly known), its position becomes less certainly known, according to the Heisenberg uncertainty principle:

$$\Delta x \Delta p \geq h/2\pi$$

where Δx is the uncertainty in position and Δp is the uncertainty in momentum, with h as Planck's constant. In a manner of speaking, the particle is in many places at the same time. In this collective state, the Cooper pair excitation energies are separated from the ground state energies by a gap which prohibits single particles from being excited if a nearly direct current field is applied. Rather, the center of mass of the electrons moves (according to the wavefunction for the Hamiltonian of the system with applied field) allowing a macroscopic current to flow. If the electron energies stay below the energy gap in the ground state, the flow undergoes no loss, being maintained indefinitely. This theory has been fairly well verfied by experimental evidence, notably that the magnetic flux quantum corresponding to superconductors equates to a charge carrier of 2e, or twice the charge of one electron.

Josephson Junctions

Presently, MEG is only possible through the extremely high gain and low noise current-to-voltage amplification of Josephson junctions (JJ), which are 1-2 nm thick insulators forming weak links between two superconductors. In addition, the JJ detects magnetic fluctuations from direct current (DC) to frequencies well above the brain's response. Classically speaking, one would expect the amplitude of the wave function of the superconducting electrons to go to zero at the insulating junction because the electrons do not conduct through an insulator. However, in terms of quantum mechanics, the solution for the wave form is a sinusoidally varying wave in the conducting region and an exponentially decaying amplitude in the junction region; classical waves can still

exist in regions where they cannot propagate. This explanation also holds true with the uncertainty principle--if the electrons truly bounced back completely from the barrier junction, then at that point they would have a momentum of zero. If the momentum is that well known, then the position would be quite uncertain, allowing some penetration into the barrier.

The useful part of this unexpected behavior is that when the junction separates two superconductors and if the junction is thin enough, then the exponentially decaying wave functions of the electrons at the two junctions will overlap. This gives a finite probability that the electron can exist inside the insulating medium, since the probability is proportional to the wave function squared. This phenomena is known as Josephson tunneling, because the superconducting electrons go through a region where classically they are forbidden to go, yielding a superconducting current. Josephson predicted that the tunneling current I is dependent on the phase difference ψ between the two wave functions of each electron on each side of the junction according to the relation (the DC Josephson equation):

$$I = I_C \sin\psi$$

where I_C is the critical current, or the maximum current that can superconduct through the junction. Any more current would conduct normally, with resistance. These single electrons would still tunnel, but not without resistance.

Superconducting Quantum Interference Devices

The Josephson junction is the heart of a SQUID in that it allows the detection of miniscule magnetic fields with a remarkable signal to noise ratio. As was pointed out earlier, more current than the critical

current in a Josephson junction conducts with resistance. According to Ohm's law, there is a voltage drop across the gap because of the resistance. Josephson predicted that this voltage is proportional to the rate of change of the phase difference ($d\psi/dt$) between the wave functions of the electrons on each side of the junction according to the relation

$$V_J = (h/4\pi e)(d\psi/dt) = (\Phi_0/2\pi)(d\psi/dt)$$

where $\Phi_0 = h/2e$ is the magnetic flux quantum. Then the total current through the junction is

$$I_J = I_C \sin\psi + (\Phi_0/2\pi R)(d\psi/dt)$$

where the second term on the right is V_J/R and typifies the regular current, R being the ohmic resistance. When the Josephson junction is set up in this manner, it acts as an extremely sensitive phase detector, the voltage across the gap being the parameter that changes and is observed to detect the change in current. This set up also acts as a current-to-voltage converter with extremely high gain (on the order of 10^7) with extremely low intrinsic noise (the only noise comes from the regularly conducting electrons, which is small because they are still so cold).

A SQUID with a single JJ is the easiest to fully describe. Two requirements must be satisfied with the single junction SQUID: the DC Josephson equation and the fact that the sum of the Josephson voltage across the junction and the voltage that might be induced by a time-varying applied flux Φ_A, along with self inductance (L_S) induced voltage must be zero (21:75):

$$V_J - d\Phi_A/dt + L_S(dI_J/dt) = 0$$

Integrating this equation and combining it with the DC Josephson equation and the other V_J equation, one obtains the SQUID equation:

$$\Phi + L_S I_C \sin(2\pi\Phi/\Phi_0) = \Phi_A$$

where Φ is the actual flux in the ring of the SQUID. From this equation, one can see that the SQUID is a non-linear measurement device that is sensitive to magnetic fields (21:76) and that because the loop's response is periodic in Φ_A with periodicity Φ_0, this sensitivity is usually expressed in units of the flux quantum Φ_0. The Josephson junction has an effective inductance which depends on the phase difference across the gap, and it is this phase difference which acts as the parameter whose electrical properties change when magnetic flux is applied within the loop of the SQUID, perhaps by the excitation current from a magnetometer or gradiometer coil. The principle of using the SQUID to detect magnetic flux rests on this phenomena.

The biomagnetometer that was used in this study utilized a DC SQUID which has two Josephson junctions in a superconducting loop. This allows higher sensitivity than just one junction, because a more direct connection with the excitation current is possible, thus introducing less intrinsic noise.

Overall Construction

The actual magnetic flux detector is a loop of superconducting wire made of niobium, as are all the other superconductors associated with the SQUID. As a magnetic field crosses the area of the loop, a current is induced in it. However, according to the Meissner effect, the current cannot exist within the superconductor because a compensating current is set up in the surface layer. It is this compensating current that is detected and measured by the SQUID.

In reality, two other superconducting loops of niobium lie between

the actual detection coil and the SQUID. These form what is known as a gradiometer, and act as spatial discriminators, selecting only magnetic fields that are close. The way they work is really very simple. The bottom coil, or farthest from the SQUID, is the magnetic detection coil and is placed so that its loop is against the head of the subject. It is wound in a certain direction, or sense. The next coil up is the same area, but wound in the opposite sense as the magnetic detection coil. This configuration is called a first order gradiometer and is insensitive to spatially uniform fields, such as the earth's magnetic field or any other strong magnetic field far away. The field is detected by both the lower and upper coils with the same magnitude, but since they are wound in the opposite sense, the signals cancel each other out in the gradiometer. The only fields detected are ones that are close and which change significantly over the space separating the two coils. Thus, this configuration detects only the first (and higher) spatial derivative of a source and hence the name first order gradiometer (see figure 21b). The configuration used in this study was a second order gradiometer--it has two magnetic detection coils, then a set of four coils wound above in the opposite sense, and finally a set of two more wound the same direction as the first set but above the second set (see figure 21c). This is just two first order gradiometers connected in series and oppositely wound. All the coils have the same area, and together provide a higher degree of spatial discrimination, detecting only the second spatial derivative and higher. A price is paid for this selective field detection however, because this decreases the sensitivity of the overall device. Even spatially changing fields are reduced in amplitude due to the finite length of the gradiometer baseline (the distance between the coils).

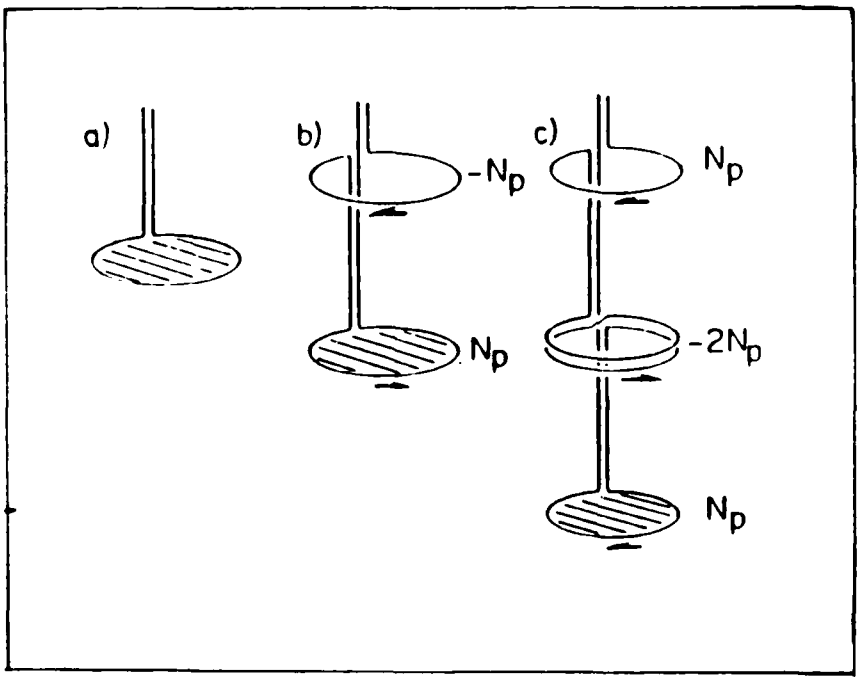

Figure 21: The Gradiometer

a) simple magnetometer

b) first order gradiometer

c) second order gradiometer

from (21:92)

The gradiometer coils and SQUID loop are constructed of niobium metal, which superconducts at 9.2^{o}Kelvin (K). Hence, to allow superconductivity, these components are submerged in a dewar of liquid helium at a temperature of 4.2^{o}K. The dewar capacity is 5 liters, and the evaporation rate is around a liter per day, so it must be filled approximately every other day. The dewar is mounted on a suspension system that allows it to be positioned and angled such that most of the brain can be measured. This is all mounted in a shielded chamber whose walls are made of 2 layers of permalloy, which is a metal with very high relative permeability (40,000 - 60,000). The high permeability metal concentrates the lines of magnetic flux. Thus, if configured as an enclosure, the inside space will have the density of lines passing through it reduced (see figure 22). This shields the inside from any magnetic noise in the outer room or building by attenuating the external field.

The biomagnetometer is a very sophisticated device capable of measuring magnetic flux on the order of femto (10^{-15}) Tesla. One must go quite deep into quantum mechanics in order to describe it accurately from a quantitative standpoint. This appendix has observed it from a qualitative aspect, proving more by common sense than mathematical rigor. A qualitative picture of superconductors and Josephson junctions was first drawn, finishing up the discussion with the overall construction of the device.

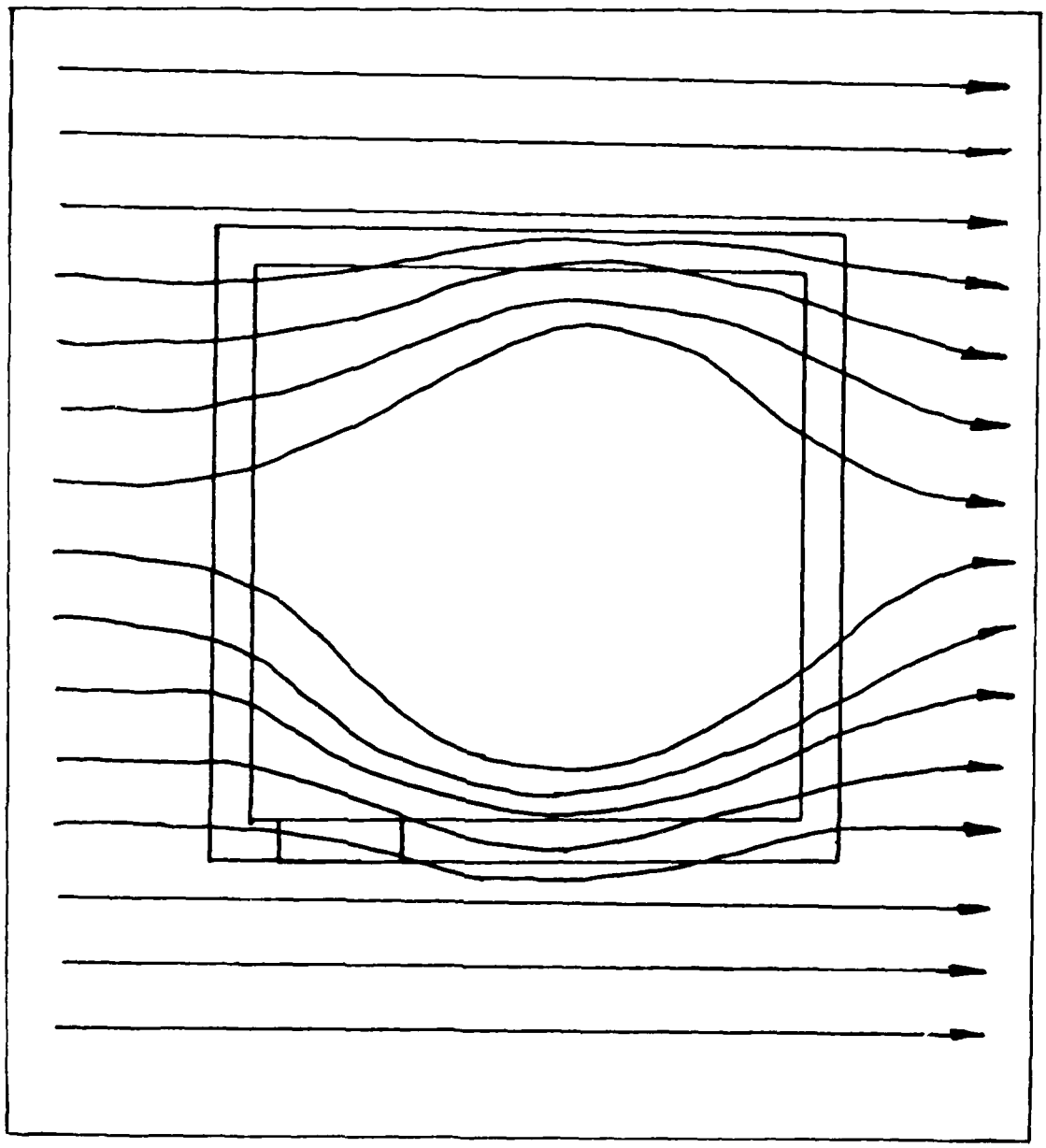

Figure 22: The Shielded Room and Its Effect
On an External Magnetic Field
(high magnitude, distant location)

Bibliography

1. Bardeen, J., Cooper, N., Schreiffer, J.R. Physical Review,106: 162 (1957), 108: 1175 (1957).

2. Bruce, V., Green, P. Visual Perception; Physiology, Psychology, and Ecology. Hillsdale NJ: Lawrence Erlbaum Assoc., 1985.

3. Desmedt, J.E. (ed.) Visual Evoked Potentials in Man: New Developments. Oxford: Clarendon Press, 1977.

4. French, A., Taylor, E. An Introduction to Quantum Physics: The MIT Indroductory Physics Series. New York: W.W. Norton & Co. 1978.

5. Grynszpan, F. "Relationship Between the Surface Electromagnetic Fields and the Electrical Activity of the Heart," Ph.D. Dissertation, University of Pennsylvania, (1971).

6. Jeffereys, D.A., Axford, J.G. "Source Locations of Pattern-Specific Components of Human Visual Evoked Potentials. I. Component of Striate Cortical Origin," Experimental Brain Research 16: 1-21 (1972).

7. Jeffereys, D.A., Axford, J.G. "Source Locations of Pattern-Specific Components of Human Visual Evoked Potentials. II. Component of Extrastriate Cortical Origin," Experimental Brain Research 16: 22-40 (1972).

8. Kalat, J.W. Biological Psychology, 2nd ed. Belmont CA: Wadsworth Publishing Co., (1984).

9. Kaufmann, L., Williamson, S.J. "Magnetic Location of Cortical Activity," Annals New York Academy of Sciences (1983).

10. Kittel, C. Introduction to Solid State Physics. 3rd ed. New York: John Wiley and Sons, 1966.

11. Liboff, R.L. Introductory Quantum Mechanics. Oakland CA: Holden Day inc., 1980.

12. Maturana, H.R., et al., "Evidence That Cut Optic Nerve Fibers in a Frog Regenerate to Their Proper Places in the Tectum," Science 130: 1709-1710 (Dec., 1959).

13. Meissner, W., Ochsenfeld, R. Naturwissenschaft 21: 787 (1933).

14. Okada, Y.C., et al. "Modulation Transfer Functions of the Human Visual System Revealed by Magnetic Field Measurements," Vision Research 22: 319-333 (1982).

15. Onnes, K.H. Akad von Wetenschappen (Amsterdam) 14: 313 (1911).

16. Roth, B.J., Wikswo, J.P. Jr. "The Magnetic Field of a Single Neuron," Biophysical Journal 48: (July 1985).

17. Schwartz, E. "Computational Anatomy and Functional Architecture of Striate Cortex: A Spatial Mapping Approach to Perceptual Coding," Vision Research 20: 645-669 (1980).

18. Schwartz, E., Tootell, R., et al. "On the Mathematical Structure of the Visuotopic Mapping of Macaque Striate Cortex," Science 227: 1065-1066 (1 March 1985).

19. Tootell, R., et al. "Deoxyglucose Analyses of Retinotopic Organization in Primate Striate Cortex," Science 218: 902-904 (26 November 1982).

20. Van Essen, D.C., et al. "The Visual Field Representation in Striate Cortex of the Macaque Monkey: Asymmetries, Anisotropies, and Individual Variablity," Vision Research 24(5): 429-448 (1984).

21. Williamson, S.J., Romani, G., Kaufman, L., Modena, I. (ed.) Biomagnetism: An Interdisciplinary Approach NATO ASI Series: Series A: Life Sciences, vol. 66. New York: Plenum Press (1982).

VITA

Lieutenant Dowler was born on 18 October 1963 in Clemson, South Carolina. In 1975 his family moved to Laurel, Maryland, where he graduated from high school at Eleanor Roosevelt Science and Technology Center in 1982. He then attended Clemson University in South Carolina where he participated in ROTC and majored in biophysics. In May of 1986 he received his Bachelor of Science degree in Physics as well as a commission in the Air Force. His first assignment was to the School of Engineering, Air Force Institute of Technology.

permanent address: 6519 Debold Rd.
Sabillasville, MD
21780

UNCLASSIFIED
SECURITY CLASSIFICATION OF THIS PAGE

REPORT DOCUMENTATION PAGE

Form Approved
OMB No. 0704-0188

1a. REPORT SECURITY CLASSIFICATION UNCLASSIFIED	1b. RESTRICTIVE MARKINGS
2a. SECURITY CLASSIFICATION AUTHORITY	3. DISTRIBUTION/AVAILABILITY OF REPORT Approved for public release; distribution unlimited.
2b. DECLASSIFICATION/DOWNGRADING SCHEDULE	
4. PERFORMING ORGANIZATION REPORT NUMBER(S) AFIT/GEP/ENP/87D-6	5. MONITORING ORGANIZATION REPORT NUMBER(S)
6a. NAME OF PERFORMING ORGANIZATION School of Engineering 6b. OFFICE SYMBOL (If applicable) AFIT/ENP	7a. NAME OF MONITORING ORGANIZATION
6c. ADDRESS (City, State, and ZIP Code) Air Force Institute of Technology (AU) Wright-Patterson AFB, Ohio 45433-6583	7b. ADDRESS (City, State, and ZIP Code)
8a. NAME OF FUNDING/SPONSORING ORGANIZATION Armstrong Aerospace Medical Research Lab 8b. OFFICE SYMBOL (If applicable) AAMRL/HEG	9. PROCUREMENT INSTRUMENT IDENTIFICATION NUMBER
8c. ADDRESS (City, State, and ZIP Code) Armstrong Aerospace Medical Research Lab Wright-Patterson AFB, Ohio 45433	10. SOURCE OF FUNDING NUMBERS PROGRAM ELEMENT NO / PROJECT NO / TASK NO / WORK UNIT ACCESSION NO

11. TITLE (Include Security Classification)
RETIONTOPIC MAPPING OF THE HUMAN VISUAL SYSTEM WITH MAGNETOENCEPHALOGRAPHY

12. PERSONAL AUTHOR(S)
Michael G. Dowler, B.S., 2d Lt, USAF

13a. TYPE OF REPORT	13b. TIME COVERED	14. DATE OF REPORT (Year, Month, Day)	15. PAGE COUNT
MS Thesis	FROM _____ TO _____	1987 December	71

16. SUPPLEMENTARY NOTATION

17. COSATI CODES			18. SUBJECT TERMS (Continue on reverse if necessary and identify by block number)
FIELD	GROUP	SUB-GROUP	Visual Perception, Visual Cortex, Optic Nerve, Biophysics, Retina, Biomagnetism, Magnetoencephalograms
06	04		
23	03		

19. ABSTRACT (Continue on reverse if necessary and identify by block number)

Thesis Chairman: James P. Mills, Lieutenant Colonel, USAF
Assistant Professor of Physics

Approved for public release: IAW AFR 190-1
31 Dec 87
Dean for Research and Professional Development
Air Force Institute of Technology (AU)
Wright-Patterson AFB OH 45433

20. DISTRIBUTION/AVAILABILITY OF ABSTRACT	21. ABSTRACT SECURITY CLASSIFICATION
☐ UNCLASSIFIED/UNLIMITED ☒ SAME AS RPT ☐ DTIC USERS	

22a. NAME OF RESPONSIBLE INDIVIDUAL	22b. TELEPHONE (Include Area Code)	22c. OFFICE SYMBOL
James P. Mills, Lieutenant Colonel, USAF	(513) 255-2012	AFIT/ENP

DD Form 1473, JUN 86 *Previous editions are obsolete.*

SECURITY CLASSIFICATION OF THIS PAGE
UNCLASSIFIED

A retinotopic mapping was verified using magnetoencephalography as the means to observe brain activity in one human subject. The stimulus consisted of 12 sectors of a hemicircle, 6 foveal and 6 peripheral out to about 17 degrees visual field angle. The sectors flashed indiviually for 63 milliseconds with an inter-stimulus-interval between .8 and 1.8 seconds. The recording computer was syncronized to the stimulus and recorded for .5 seconds after onset of stimulus. Thirty averages were taken for each stimulus section, for each of about 45 grid points on the scalp.

The sectors were localized to distinct points in the primary visual cortex (area 17). The results did not verify the cruciform model of retinotopic mapping nor the theory that more visually eccentric stimuli produce deeper responses. The data seem to suggest a different type of mapping for foveal stimuli than peripheral, but this could also be due to the fold structure of the primary visual cortex.

END
DATE
FILMED
3-1988
DTIC